Лазерное воздействие на металлы: физика и технологии

Н.А. Иногамов[1], В.В. Жаховский[2,1], К.П. Мигдал[2,1], Д.К. Ильницкий[2,1]

[1]ИТФ им. Л.Д. Ландау РАН

[2]ВНИИА им. Н. Л. Духова, Росатом

Сообщение на совещании «Исследования в области физики высоких плотностей энергии лазерными и электрофизическими методами» 2-го апреля 2018 г.

Focusing conditions:

- Fluence absorbed from ~0.01 to ~1 J/cm^2
- radius of focal spot R_L :
- $R_L >> \lambda$
- $R_L \sim \lambda$
- beam structure :
- F=max in center
- F=0 in center

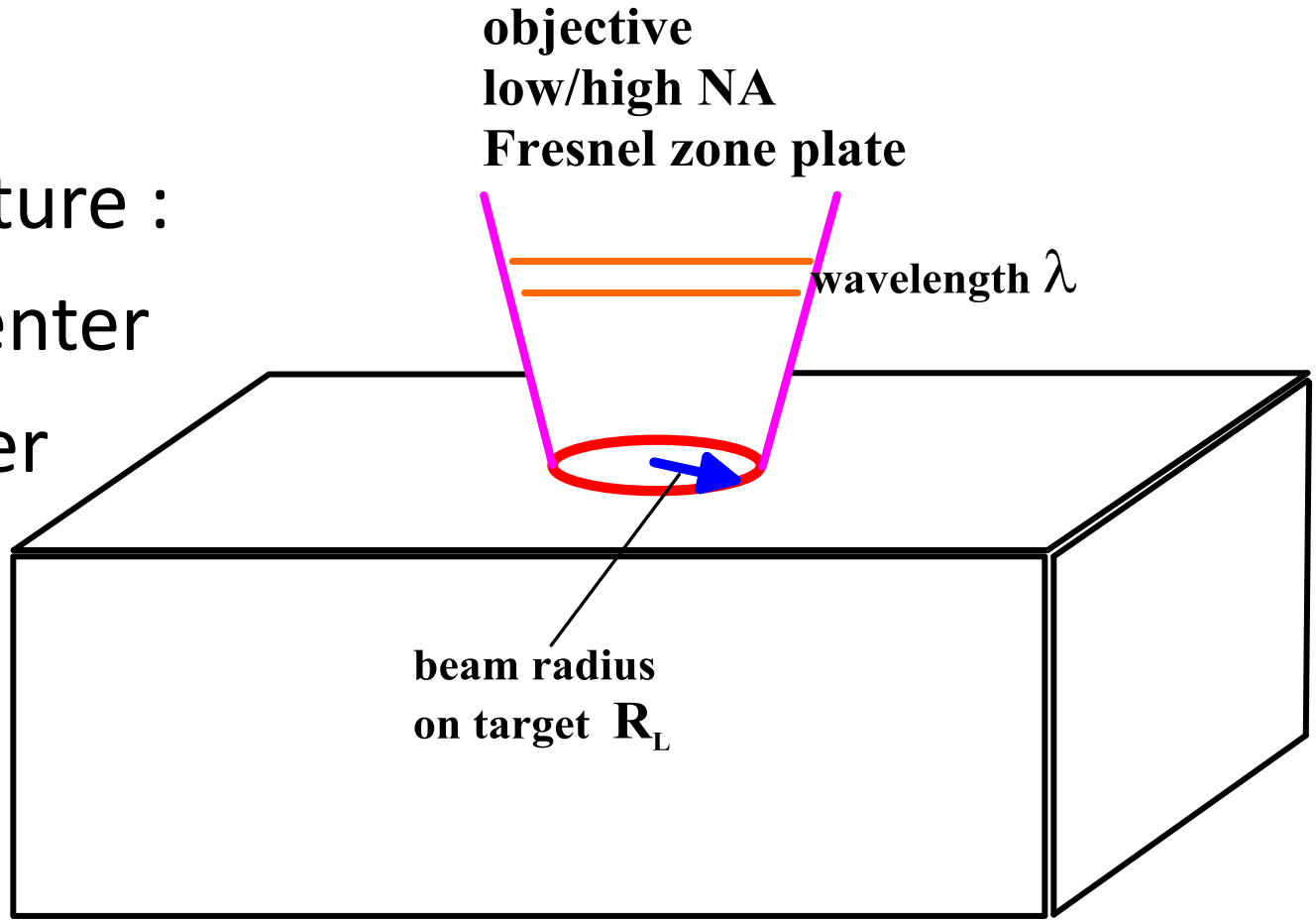

Laser-matter interaction

- Targets: bulk targets, film targets
- Thin films – thick films
  - Free standing films, supported films
  - Laminates
  - Nanoparticles formation
  - Powders, sintering

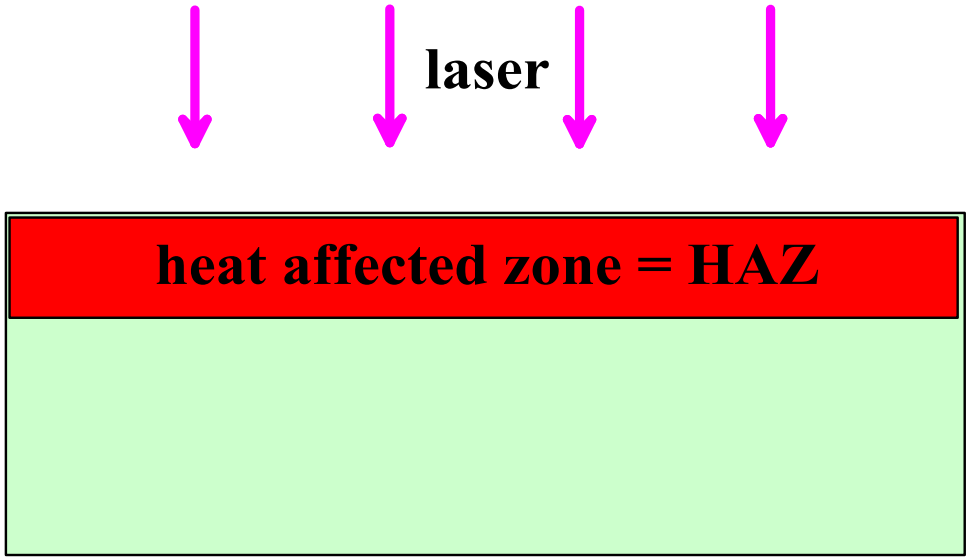

Short pulses 1 ps and less. Film is **thin** if HAZ is thinner than d_f – film thickness
Thickness of HAZ d_T is from 10s to 100s nm in metals

Thick films are if df is 2-5 times thicker than HAZ

Bulk targets if film is 7-10 times and more thicker than HAZ

Blistering of thin films + tight focusing

tight focusing is diffraction limited focusing
then for IR-UV light a radius of focal spot is ~ 1 μm

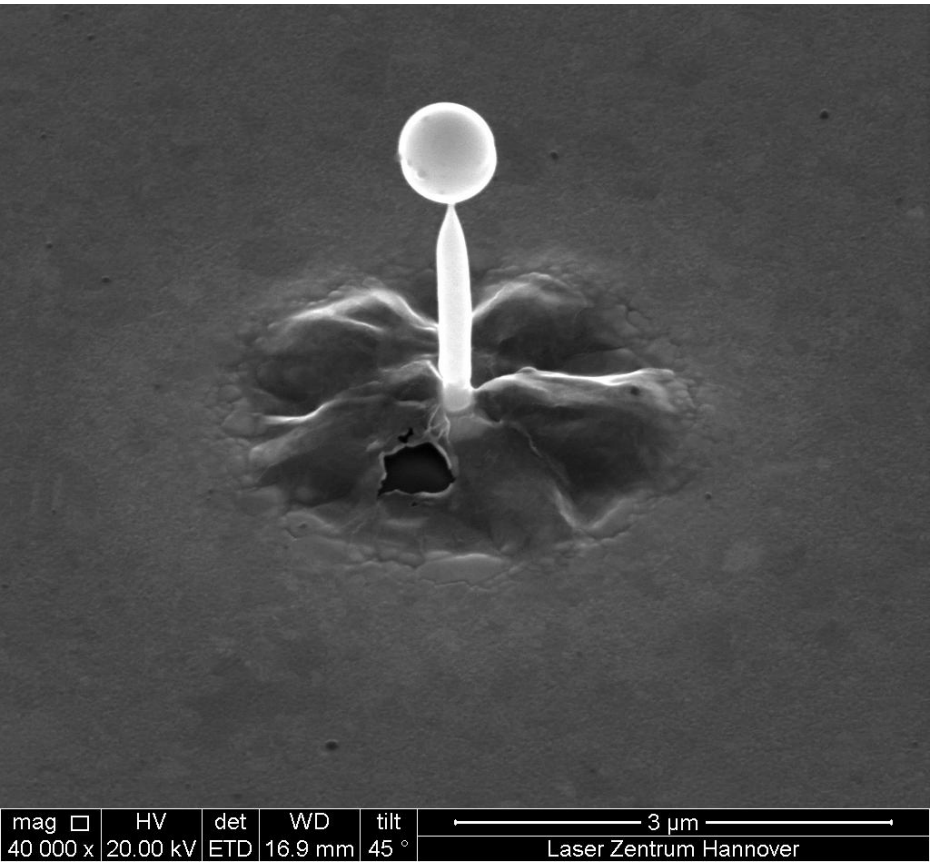

B. Chichkov et al.,
2004-2016. Size =
see the scale bar

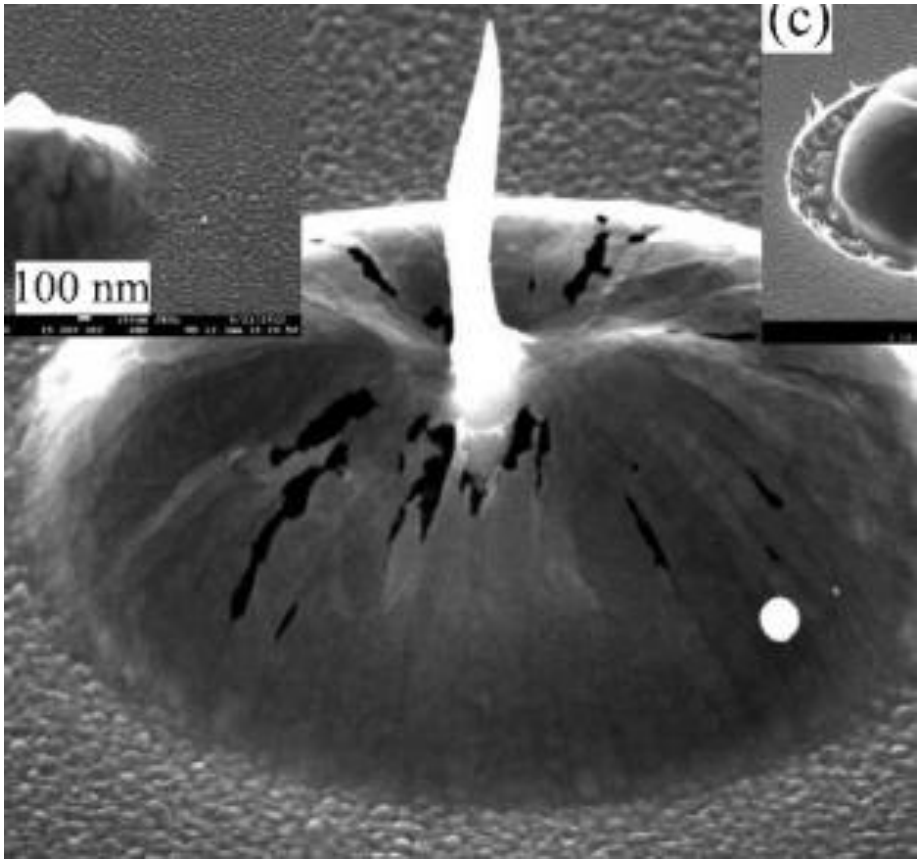

Danilov et al.,
JETP Lett. (2016);
Danilov,...,INA,
JETP Lett. v. 104, p. 759 (2016)

Приложения

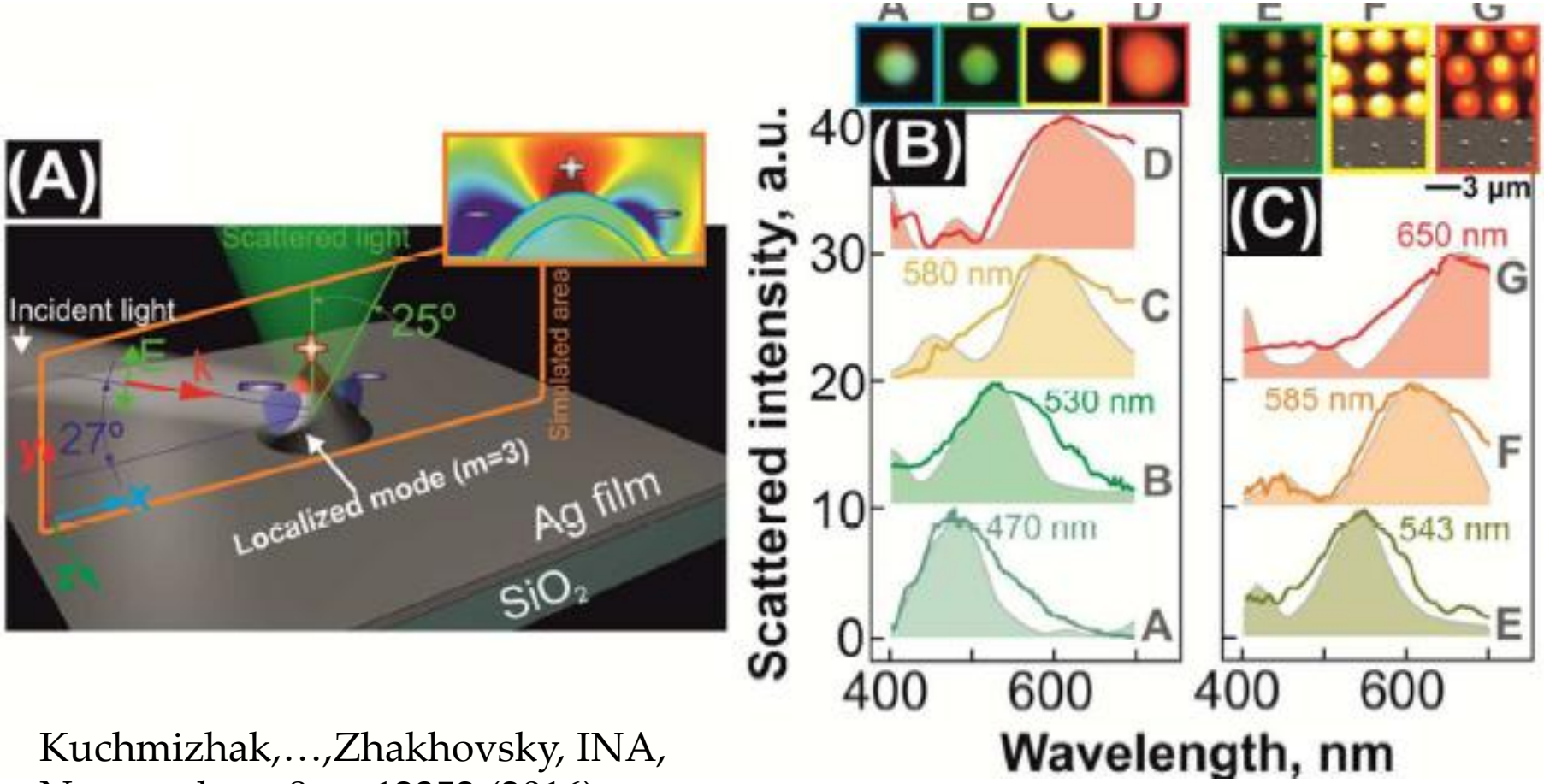

Kuchmizhak,…,Zhakhovsky, INA, Nanoscale, v. 8, p. 12352 (2016)

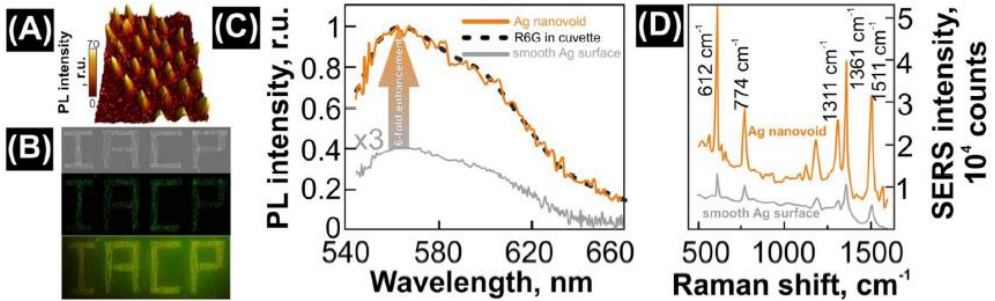

Приложения

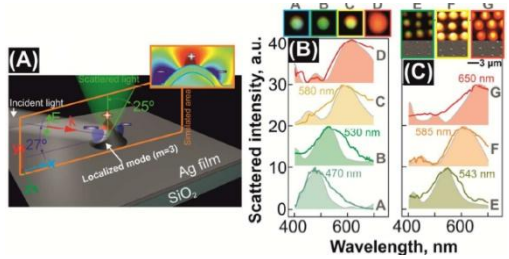

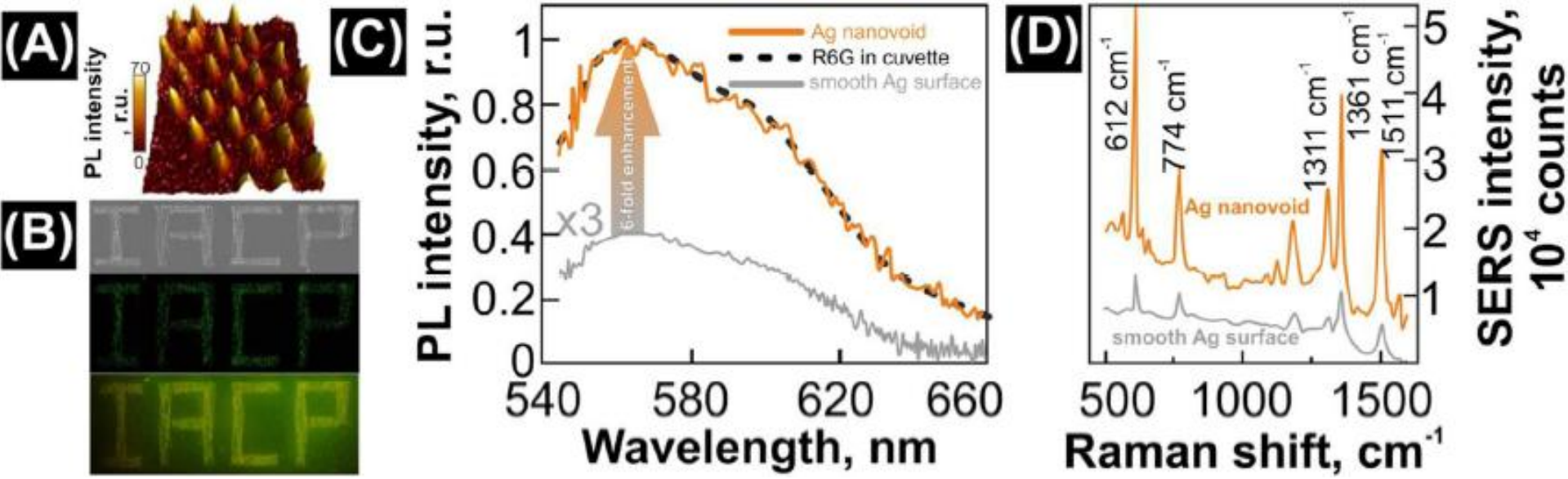

Kuchmizhak,…,Zhakhovsky, INA, Nanoscale, v. 8, p. 12352 (2016)

IACP = Institute of Automation and Control Processes

Физика воздействия лазера на металл

$$\rho(z^o, t)\frac{\partial z(z^o, t)}{\partial z^o} = \rho^o, \quad \frac{\partial z(z^o, t)}{\partial t} = u(z^o, t),$$

$$\rho^o\frac{\partial u}{\partial t} = \frac{\partial P(z^o, t)}{\partial z^o}, \quad P = P_i + P_e,$$

$$\rho^o\left(\frac{E_e}{\rho}\right)_t = -q' - \frac{\rho^o}{\rho}\alpha(T_e - T_i) + \frac{\rho^o}{\rho}Q - P_e\frac{\partial u}{\partial z^o},$$

$$\rho^o\frac{\partial(E_i/\rho)}{\partial t} = \frac{\rho^o}{\rho}\alpha(T_e - T_i) - P_i\frac{\partial u}{\partial z^o},$$

Физика воздействия лазера на металл

$$\rho(z^o,t)\frac{\partial z(z^o,t)}{\partial z^o} = \rho^o, \quad \frac{\partial z(z^o,t)}{\partial t} = u(z^o,t),$$

$$\rho^o\frac{\partial u}{\partial t} = \frac{\partial P(z^o,t)}{\partial z^o}, \quad P = P_i + P_e,$$

$$\rho^o\left(\frac{E_e}{\rho}\right)_t = -q' - \frac{\rho^o}{\rho}\alpha(T_e - T_i) + \frac{\rho^o}{\rho}Q - P_e\frac{\partial u}{\partial z^o},$$

$$\rho^o\frac{\partial(E_i/\rho)}{\partial t} = \frac{\rho^o}{\rho}\alpha(T_e - T_i) - P_i\frac{\partial u}{\partial z^o},$$

Уравнение термодинамического состояния с учетом двух-температурных состояний

Физика воздействия лазера на металл

$$\rho(z^o,t)\frac{\partial z(z^o,t)}{\partial z^o} = \rho^o, \quad \frac{\partial z(z^o,t)}{\partial t} = u(z^o,t),$$

$$\rho^o\frac{\partial u}{\partial t} = \frac{\partial P(z^o,t)}{\partial z^o}, \quad P = P_i + P_e,$$

$$\rho^o\left(\frac{E_e}{\rho}\right)_t = -q' - \frac{\rho^o}{\rho}\alpha(T_e - T_i) + \frac{\rho^o}{\rho}Q - P_e\frac{\partial u}{\partial z^o},$$

$$\rho^o\frac{\partial(E_i/\rho)}{\partial t} = \frac{\rho^o}{\rho}\alpha(T_e - T_i) - P_i\frac{\partial u}{\partial z^o},$$

Электрон-ионный обмен энергией

Физика воздействия лазера на металл

$$\rho(z^o,t)\frac{\partial z(z^o,t)}{\partial z^o} = \rho^o, \quad \frac{\partial z(z^o,t)}{\partial t} = u(z^o,t),$$

$$\rho^o\frac{\partial u}{\partial t} = \frac{\partial P(z^o,t)}{\partial z^o}, \quad P = P_i + P_e,$$

$$\rho^o\left(\frac{E_e}{\rho}\right)_t = -q' - \frac{\rho^o}{\rho}\alpha(T_e - T_i) + \frac{\rho^o}{\rho}Q - P_e\frac{\partial u}{\partial z^o},$$

$$\rho^o\frac{\partial(E_i/\rho)}{\partial t} = \frac{\rho^o}{\rho}\alpha(T_e - T_i) - P_i\frac{\partial u}{\partial z^o},$$

Электронная теплопроводность
с учетом двух-температурных состояний

$$q = -\frac{\rho\kappa}{\rho^o}\frac{\partial T_e}{\partial z^o}$$

Преодоление разрыва между наличными на сегодня ресурсами и требуемыми

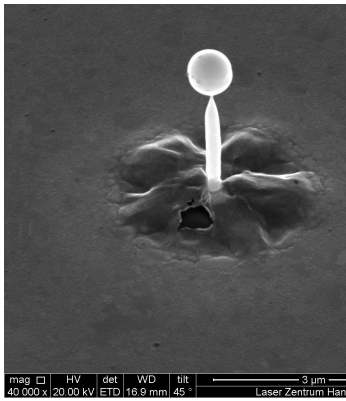

- 3000*3000*(50+3*50)*60 = 10^11 атомов
- (0.1-1)*10^9 = limit
- Как обойти?
- 1) разделить на начальную стадию ~df/cs и последующую RL/Vf
- 2) начальную стадию описать с помощью 2Т-ГД кода (двухтемпературный гидрокод) → тогда мы знаем Vf в эксперименте
- 3) полет пленки после ее отрыва от подложки моделировать посредством МД

Преодоление разрыва между наличными на сегодня ресурсами и требуемыми

- 3000*3000*(50+3*50)*60 = 10^11 атомов
- (0.1-1)*10^9 = limit
- Как обойти?
- 4) МД-МК код. МК=Монте-Карло = вариация коэффициента теплопроводности каппа
- 5) МД полет. Использование теории подобия Vf это скорость пленки, она же Vc(t=0)

$$v_\sigma = 2\sqrt{\sigma/(\rho d_f)} = 46\,[\sigma/(1000\mathrm{dyne/cm})]^{1/2}\,[\rho/(19.3\mathrm{g/cm^3})]^{-1/2}\,[d_f/(100\mathrm{nm})]^{-1/2}\ \ [\mathrm{m/s}]$$

$$v_\chi = \chi/R_L = 100\,[\chi/(1\,\mathrm{cm}^2/\mathrm{s})]\,/\,[R_L/(1\,\mu\mathrm{m})]\ \ [\mathrm{m/s}], \qquad v_{0\chi} = v_c(t=0)/v_\chi.$$

Преодоление разрыва между наличными на сегодня ресурсами и требуемыми

- 2Т-ГД код → тогда мы знаем Vf в эксперименте

$$v_\sigma = 2\sqrt{\sigma/(\rho d_f)} = 46\,[\sigma/(1000\mathrm{dyne/cm})]^{1/2}\,[\rho/(19.3\mathrm{g/cm^3})]^{-1/2}\,[d_f/(100\mathrm{nm})]^{-1/2}\ \ [\mathrm{m/s}]$$

$$v_\chi = \chi/R_L = 100\,[\chi/(1\,\mathrm{cm}^2/\mathrm{s})]\,/\,[R_L/(1\,\mu\mathrm{m})]\ \ [\mathrm{m/s}], \qquad v_{0\chi} = v_c(t=0)/v_\chi.$$

- Получили экспериментальные значения Vf/Vsigma, Vf/Vchi : капиллярное число и тепловое число
- df в МД на порядок меньше → Vsigma и Vf в МД в sqrt(10) раз больше
- RL в МД в 5 раз меньше. Уменьшаем chi так, чтобы тепловое число Vf/Vchi было как в опыте

Large scale MD: few 100s mln atoms

MD = Molecular Dynamics. The code includes Monte-Carlo heat transfer, thus it describes cooling and thus it describes freezing = re-solidification !
Solid is shown by green colors, while **molten gold by red** colors

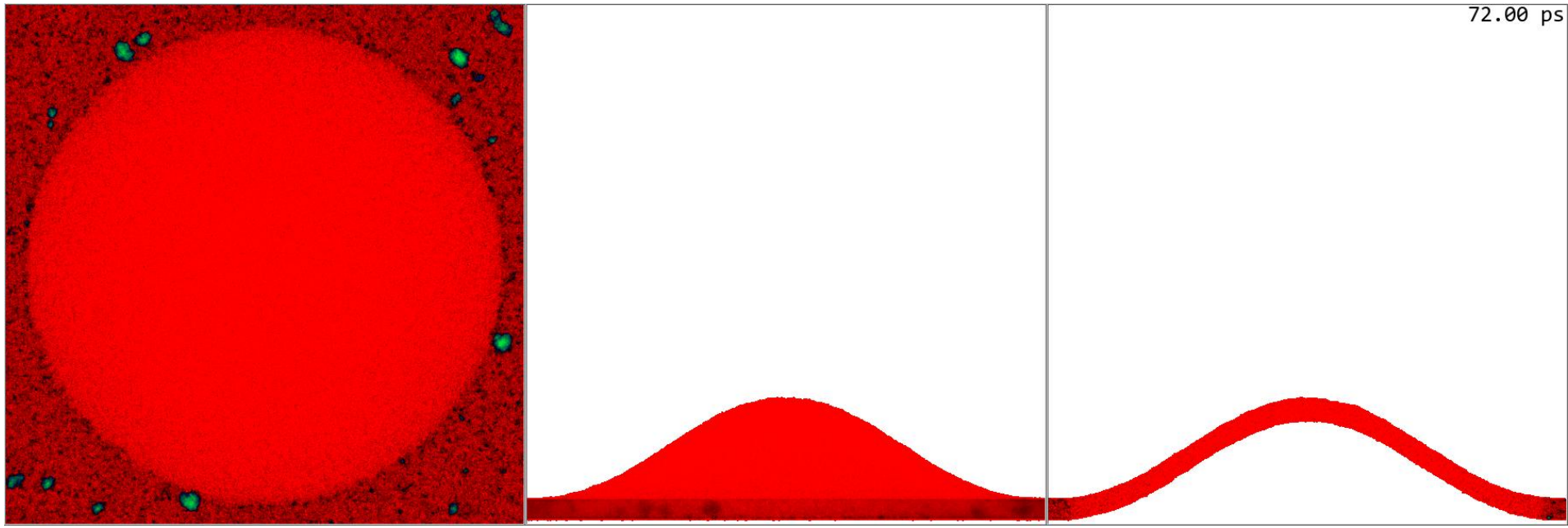

ИНА, Жаховский, Письма ЖЭТФ, т.100, с.6 (2014)
ИНА и др., ЖЭТФ, т.147, с.20 (2015)
INA et al., Appl. Phys. A 122:432 (2016)
INA et al., Nanoscale Res. Lett. 11:177 (2016)
Анисимов,ИНА и др., Квант. Электроника т.47, с.509 (2017)

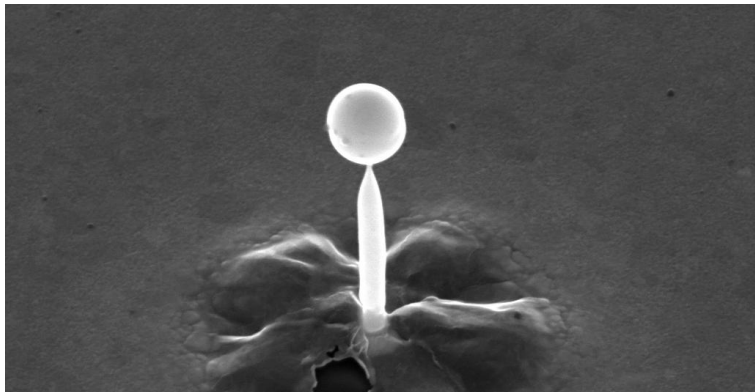

Large scale MD: few 100s mlns of atoms

Danilov,...,Zhakhovsky,INA, JETP Lett. v. 104, p. 759 (2016)

Delayed freezing (slow freezing) →
then liquid has opportunity to escape solidification.
Fate of liquid jet is demonstrated

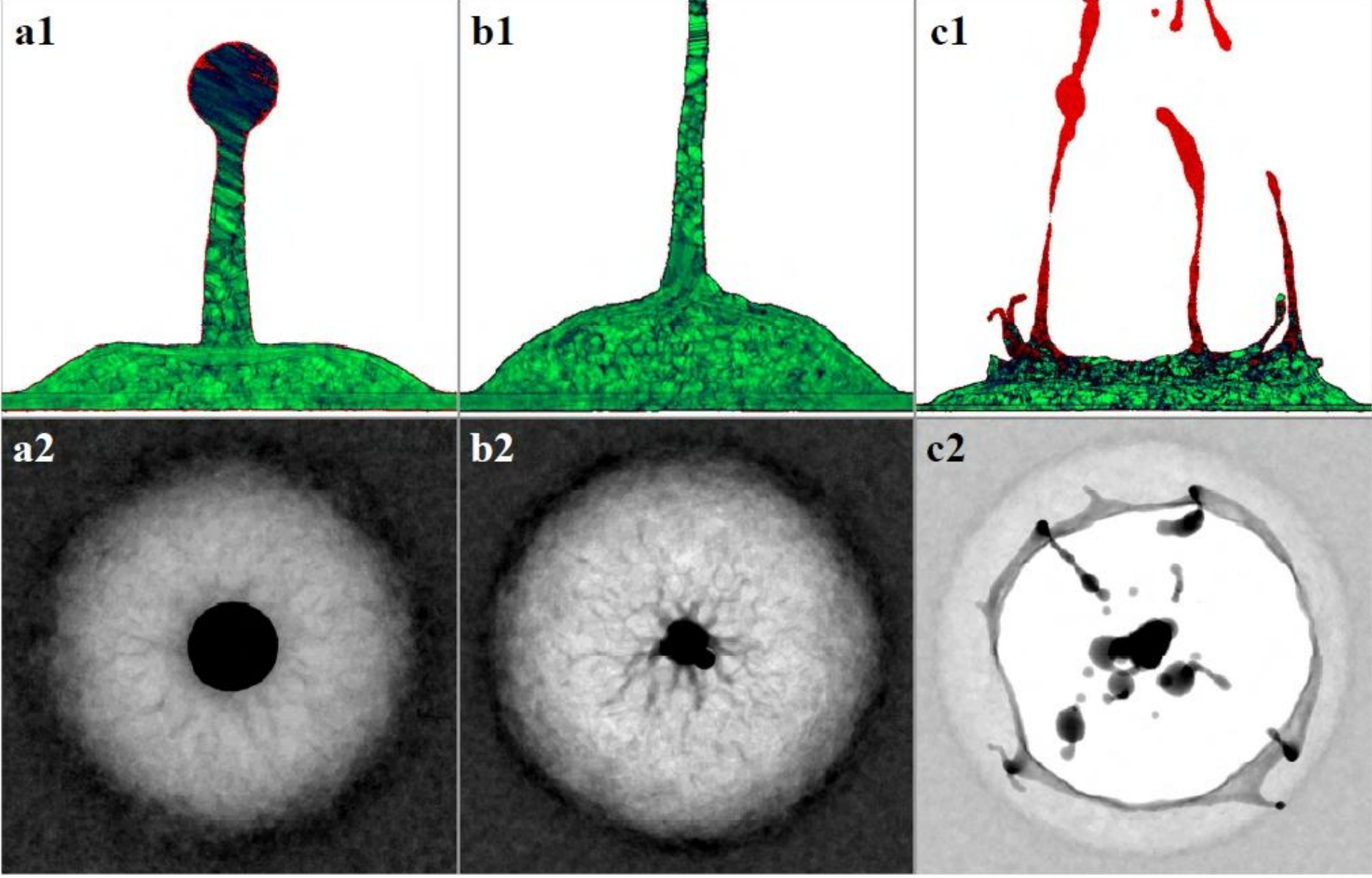

In the cases with large spot or high energies, the shell cannot be frozen fast → then a hole (films) or crater (bulk) remain. They are encircled by a frozen rim = Only the rim has time to be solidified

Danilov,...,Zhakhovsky,INA, JETP Lett. v. 104, p. 759 (2016)

Rupture of a jet and solidification of the tip

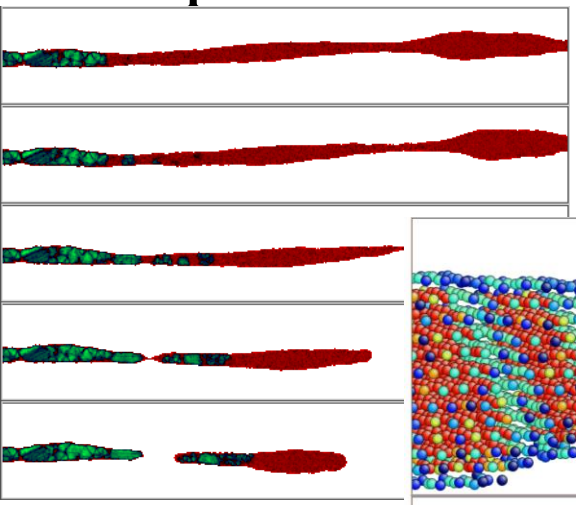

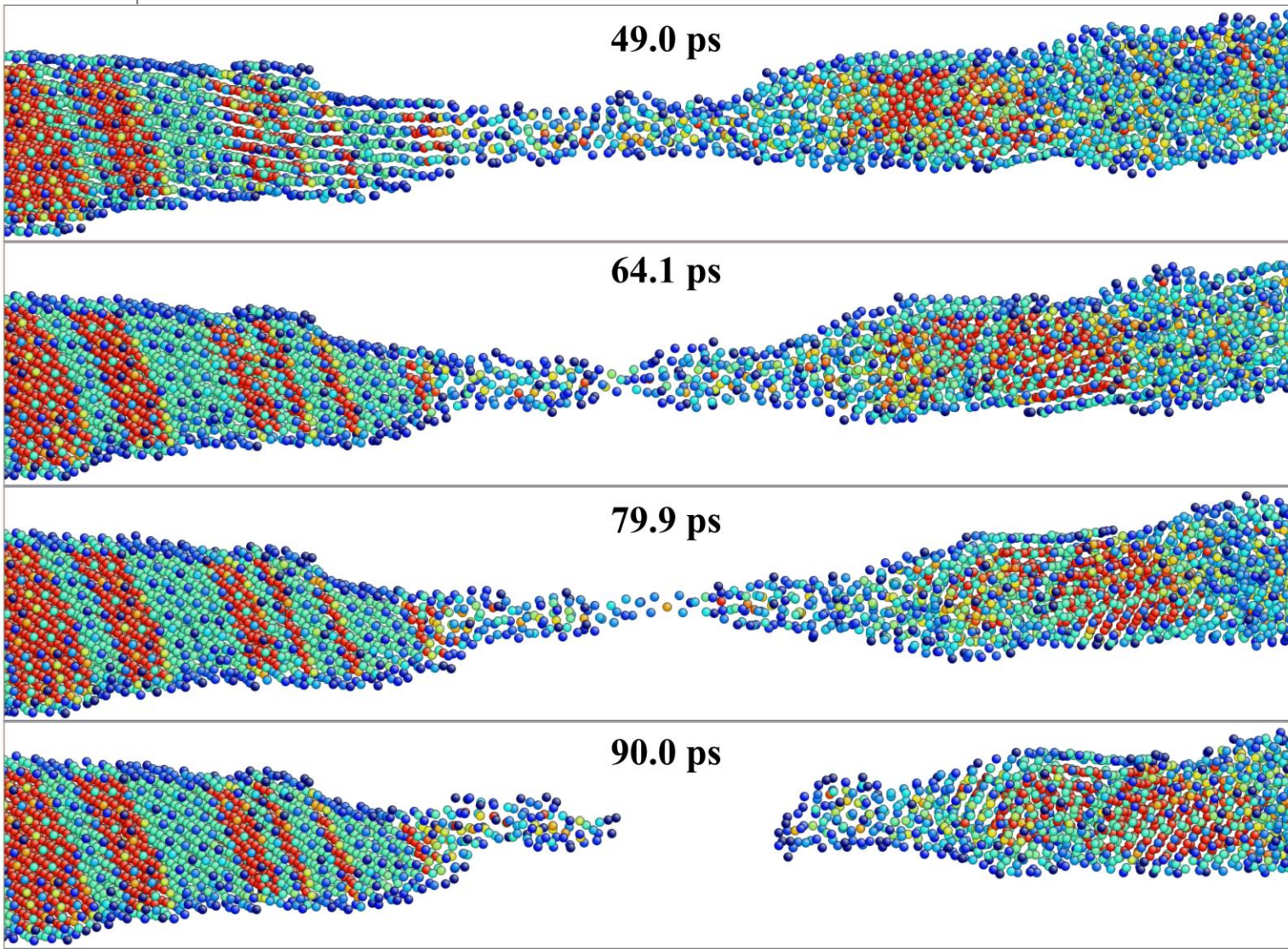

Rupture of a jet and solidification of the tip

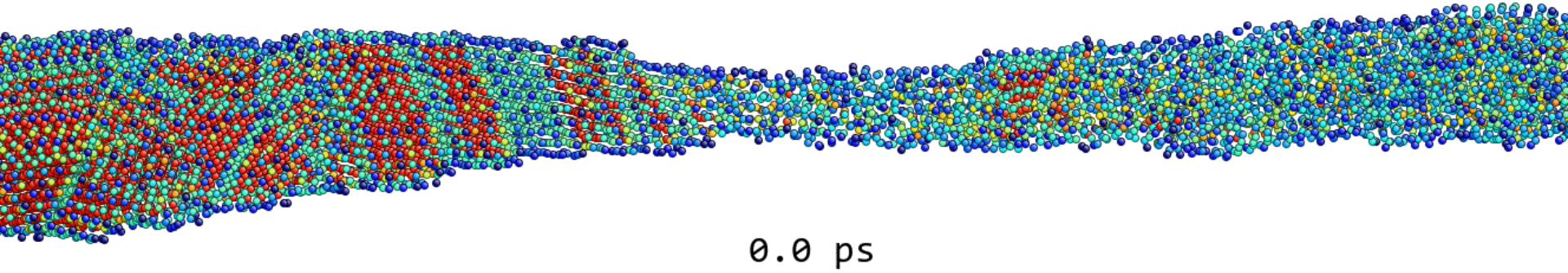

Анисимов, ИНА и др., Квант. Электроника т.47, с.509 (2017);
INA, Zhakhovsky, Lobachevskii Journal of Mathematics, v. 38, p. 914 (2017);
arXiv:1701.04576

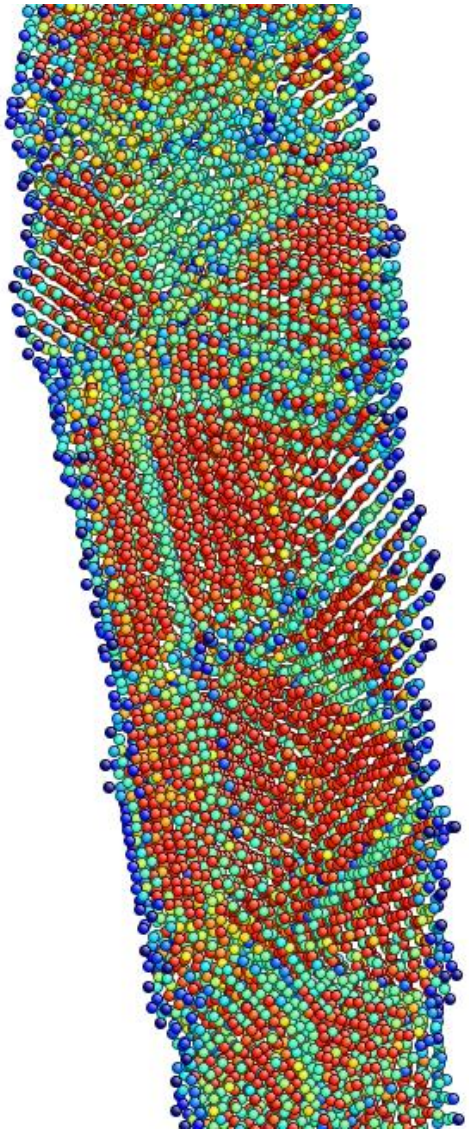

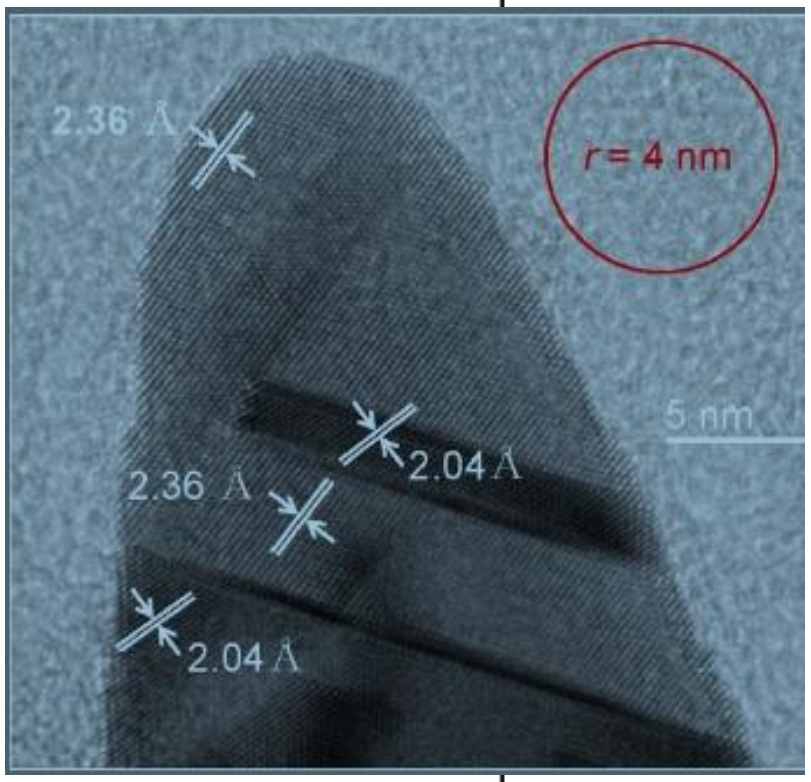

Nanocrystallin structure in our simulation and in experiments Nakata et al., Appl. Surf. Sci. (2013)

Rupture of a jet and solidification of the tip

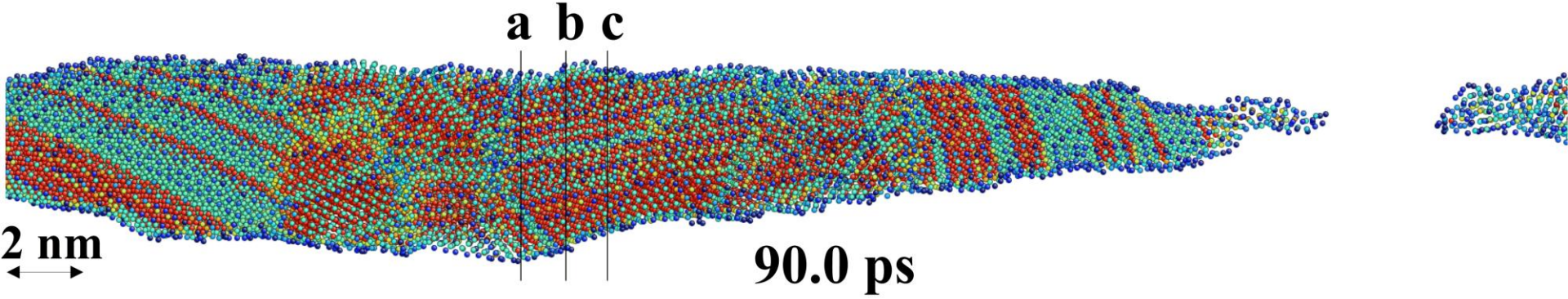

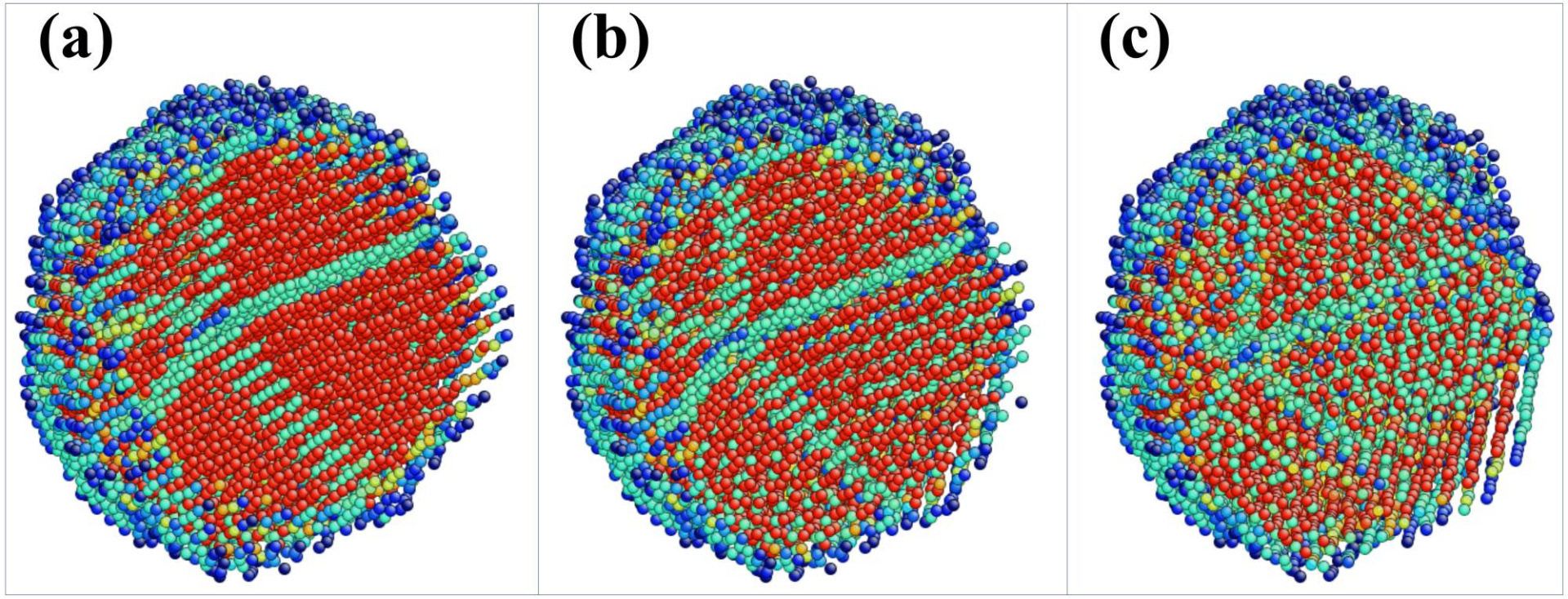

The five-fold = icosahedral symmetry seen also in foam threads by Wu, Zhigilei (2016)

Свободновисящие пленки

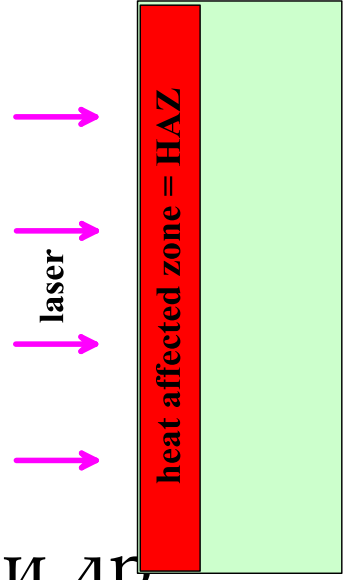

Теперь БЕЗ подложки: воздух с двух сторон

Пример допороговый. Вид по нормали к пленке

Опыт выполнен во Владивостоке Кучмижак и др.

ИАПУ ДВО РАН (инст. автоматики и процессов управления)

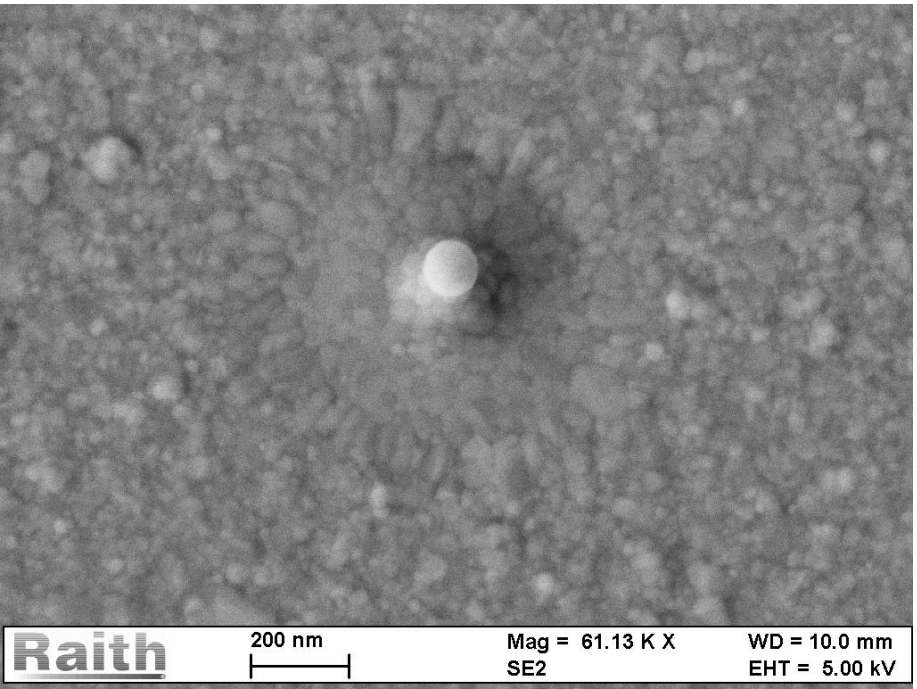

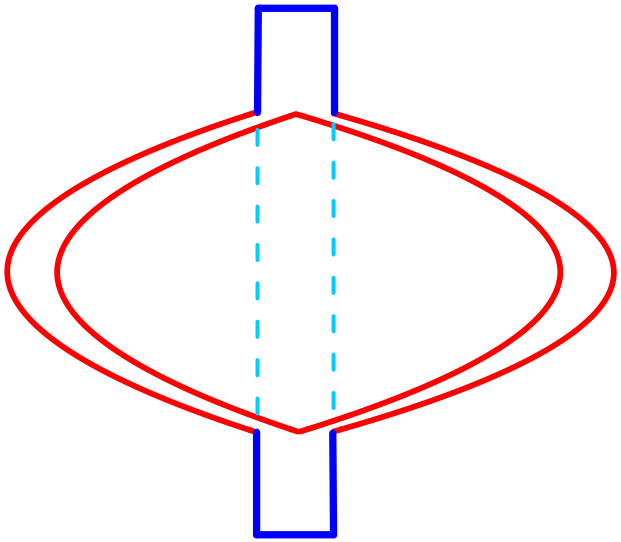

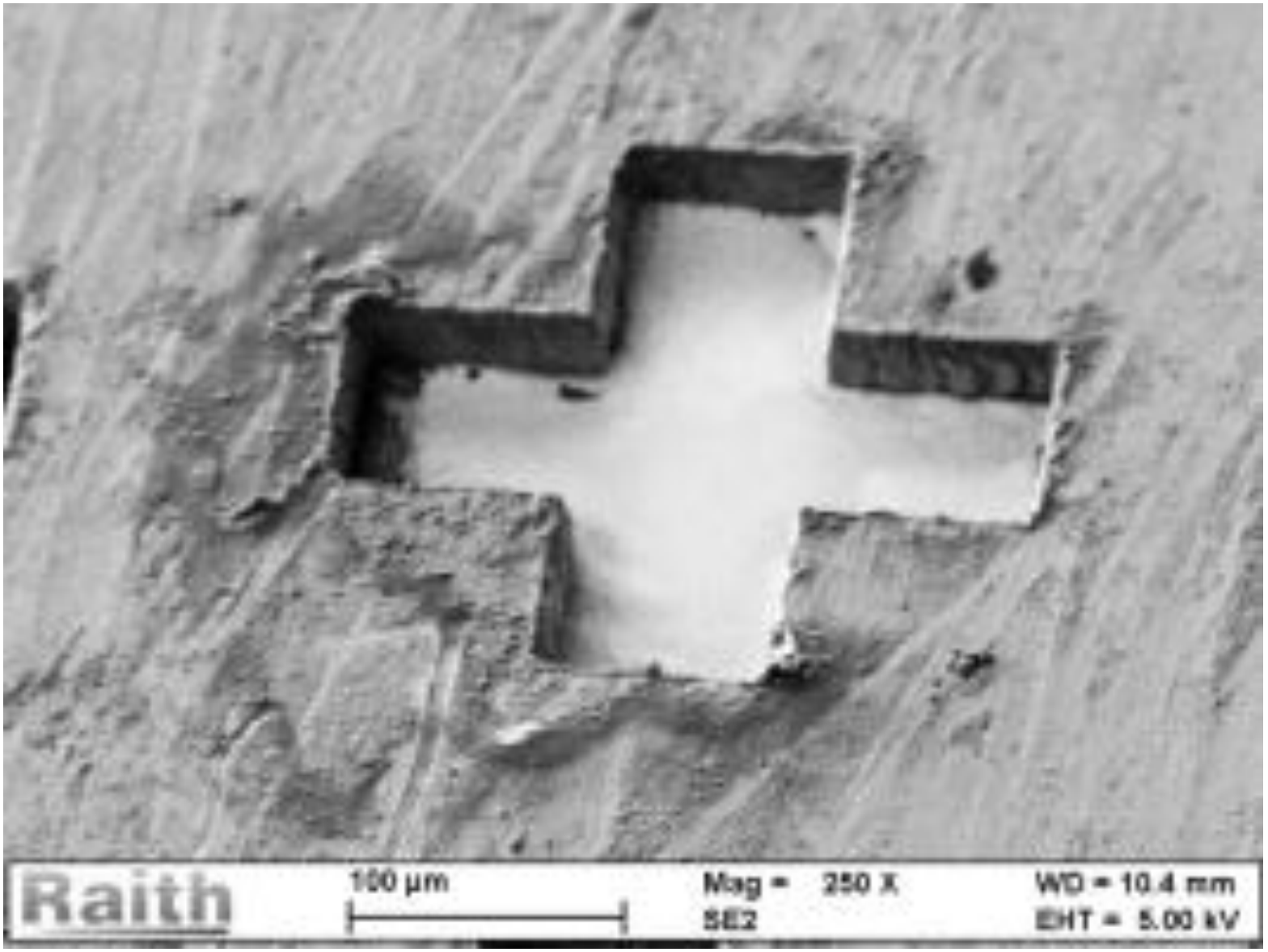
Raith
100 µm
Mag = 250 X
SE2
WD = 10.4 mm
EHT = 5.00 kV

Свободновисящие пленки

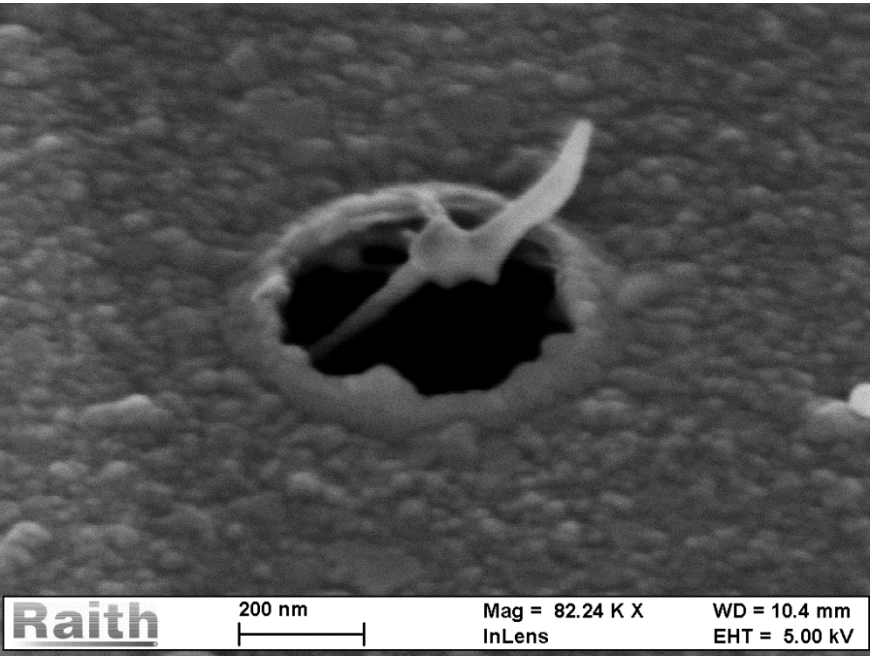

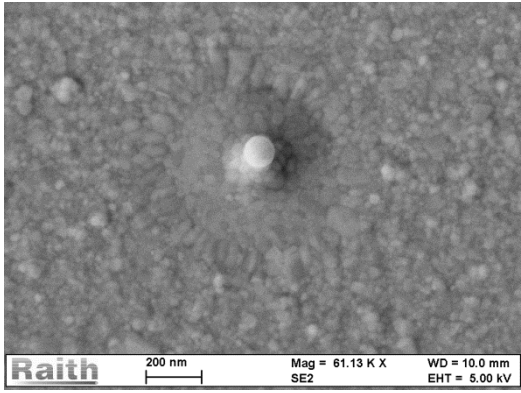

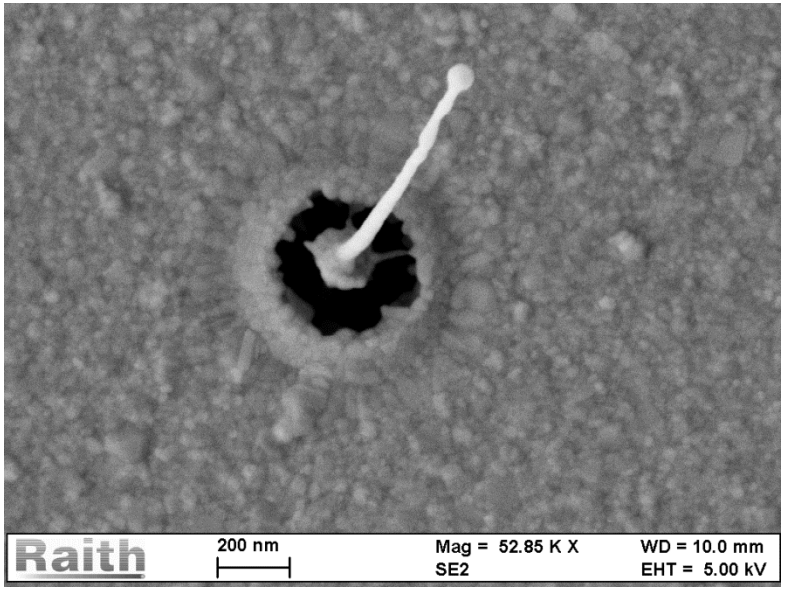

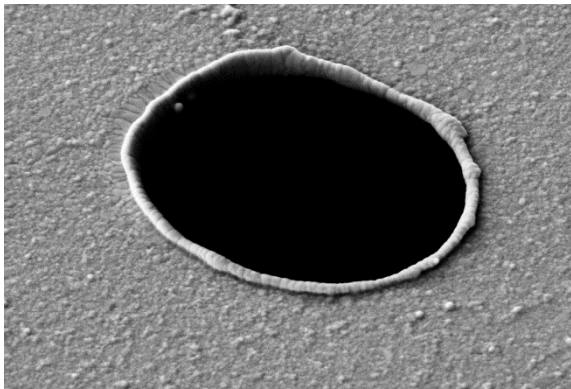

The free-standing case. Red=liquid, **green=solid**

- Shell (two of them) forms from free-standing film
- The shell survive in spite of hard bombardment by fragments of foam decomposition
- Capillarity stops and return back the shell, but it cannot stop the jet formed thanks to Rayleigh-Taylor type of jetting. Solidification freezes liquid. Rayleigh-Plateau separation of droplets

INA,Zhakhovsky,Khokhlov, J.Phys.:Conf.Ser., v.946, 012008 (2018)

The free-standing case

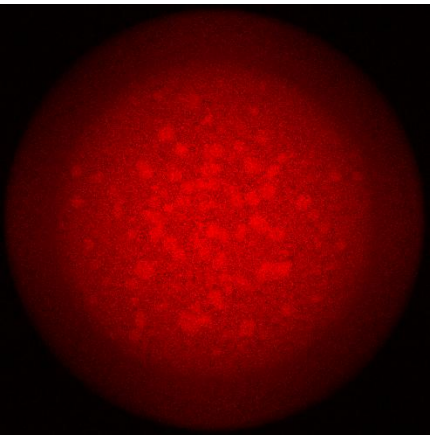
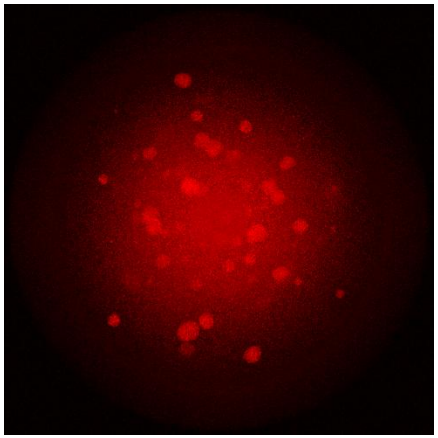
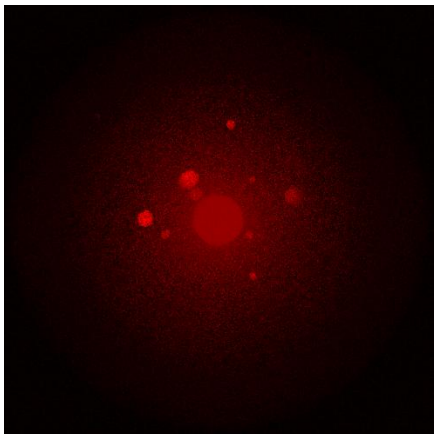
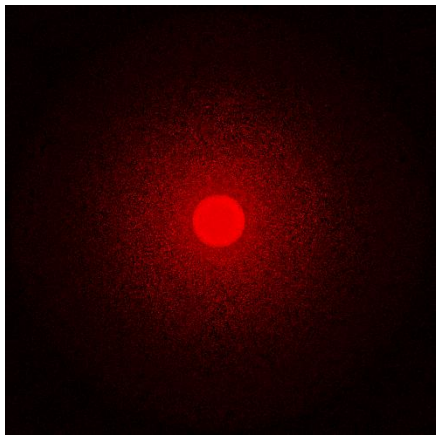

- In the previous page the side view onto breaking free-standing shell was shown
- We saw a struggle between inertia v. capillarity
- We saw how freezing stops moving liquid in its motion
- Here the view from above is given.
- This is temperature field: more red are hotter. The bright spots are droplets bombarding the shell from inside

The free-standing case

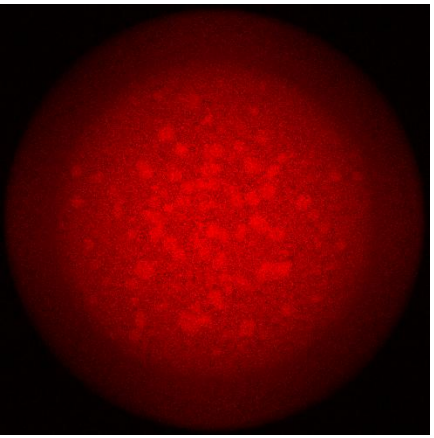
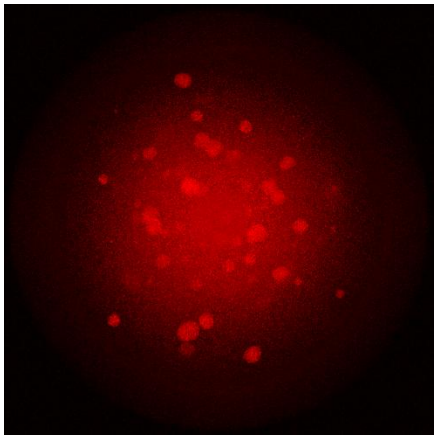
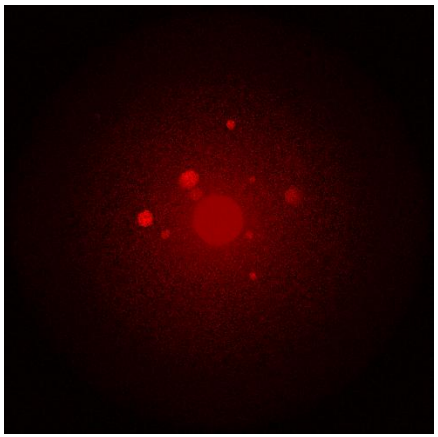
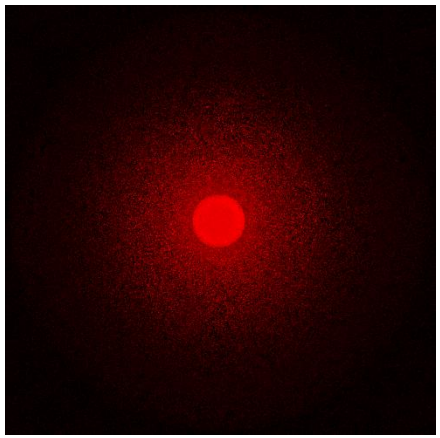

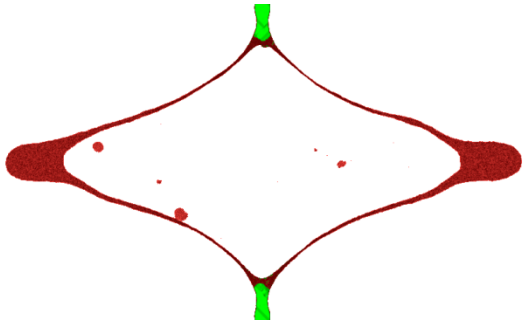

ELBRUS 2017 IOP Publishing
IOP Conf. Series: Journal of Physics: Conf. Series **946** (2018) 012008 doi:10.1088/1742-6596/946/1/012008

Laser ablation caused by geometrically constrained illumination and inventive target design

N A Inogamov[1,2], V V Zhakhovsky[2,1] and V A Khokhlov[1]

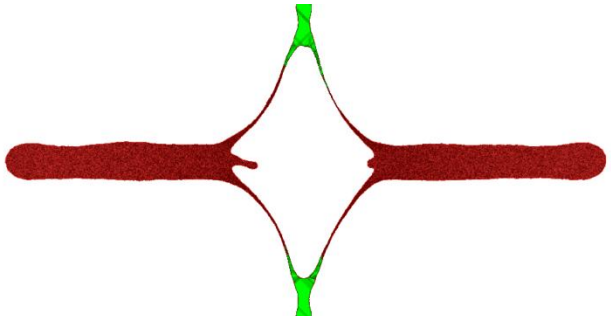

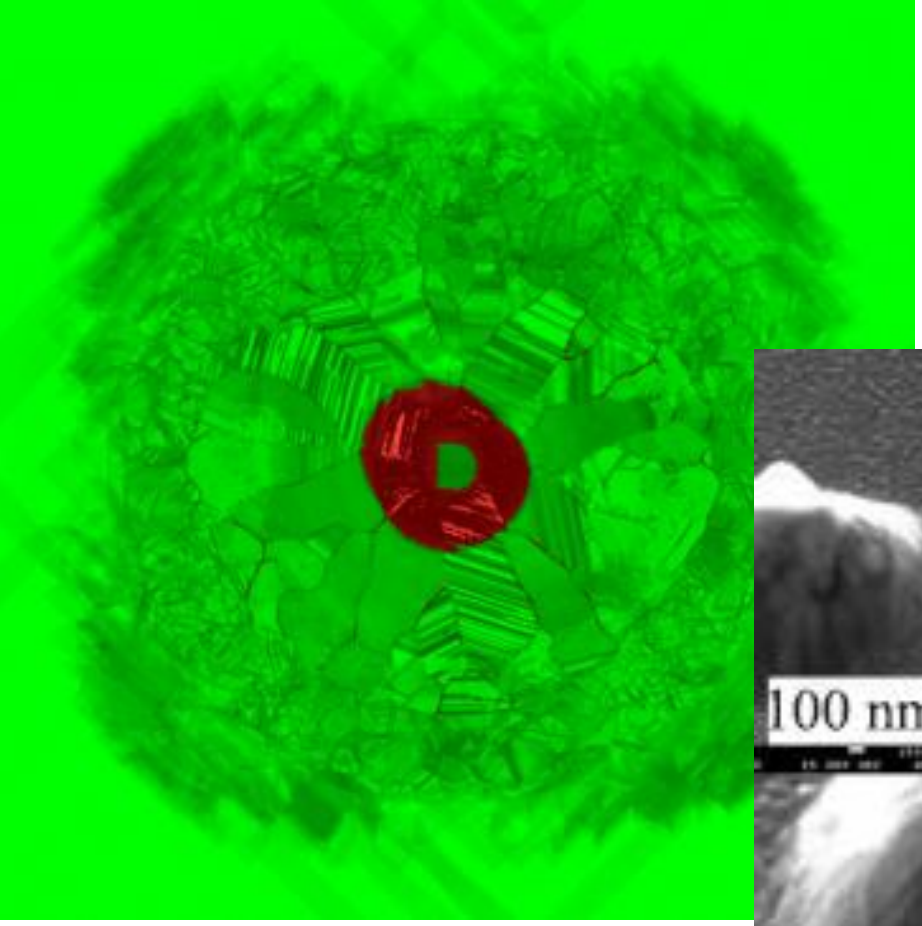

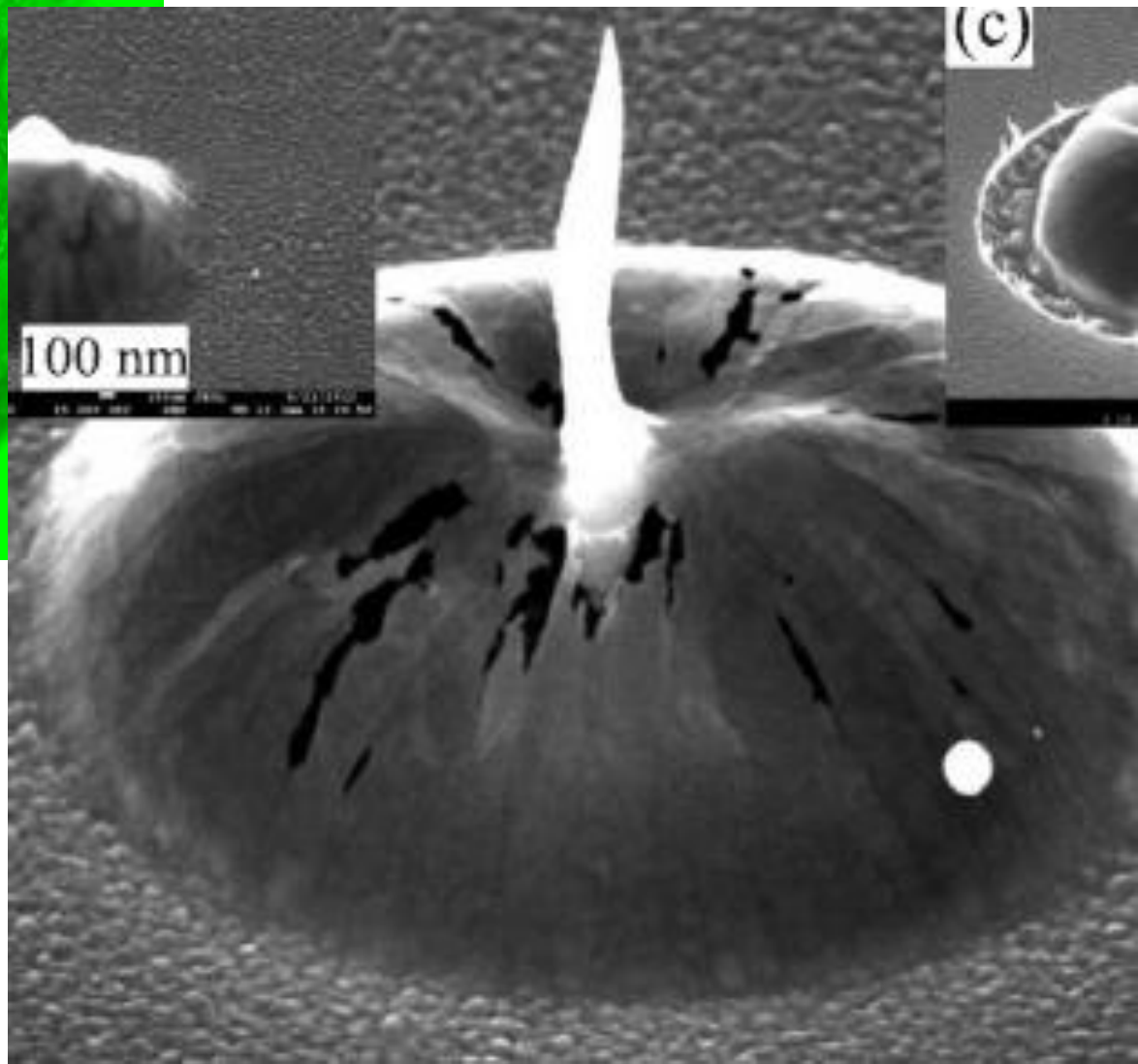

Danilov et al., JETP Lett. (2016)
The puzzle of formation of lamellated crystallites is solved:
INA,Zhakhovsky,Khokhlov,
J.Phys.:Conf.Ser.,
v.946, 012008 (2018)

Focusing conditions:

- fluence
- radius of focal spot RL
- $R_L >> \lambda$
- $R_L \sim \lambda$

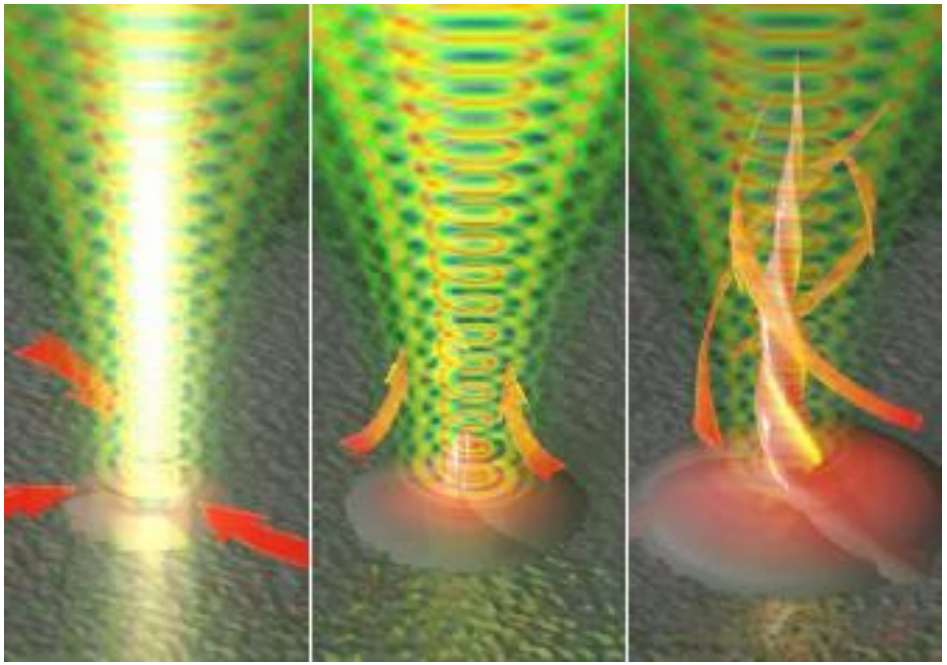

Taken from arXiv 1702.07891 by Syubaev et al.

- beam structure:
- Gaussian
- Hermite-Gaussian
- Laguerre-Gaussian
- Spiral Fresnel Zone Plate (SFZP) – toroidal intensity distribution

Разница между центральным и кольцевым воздействием

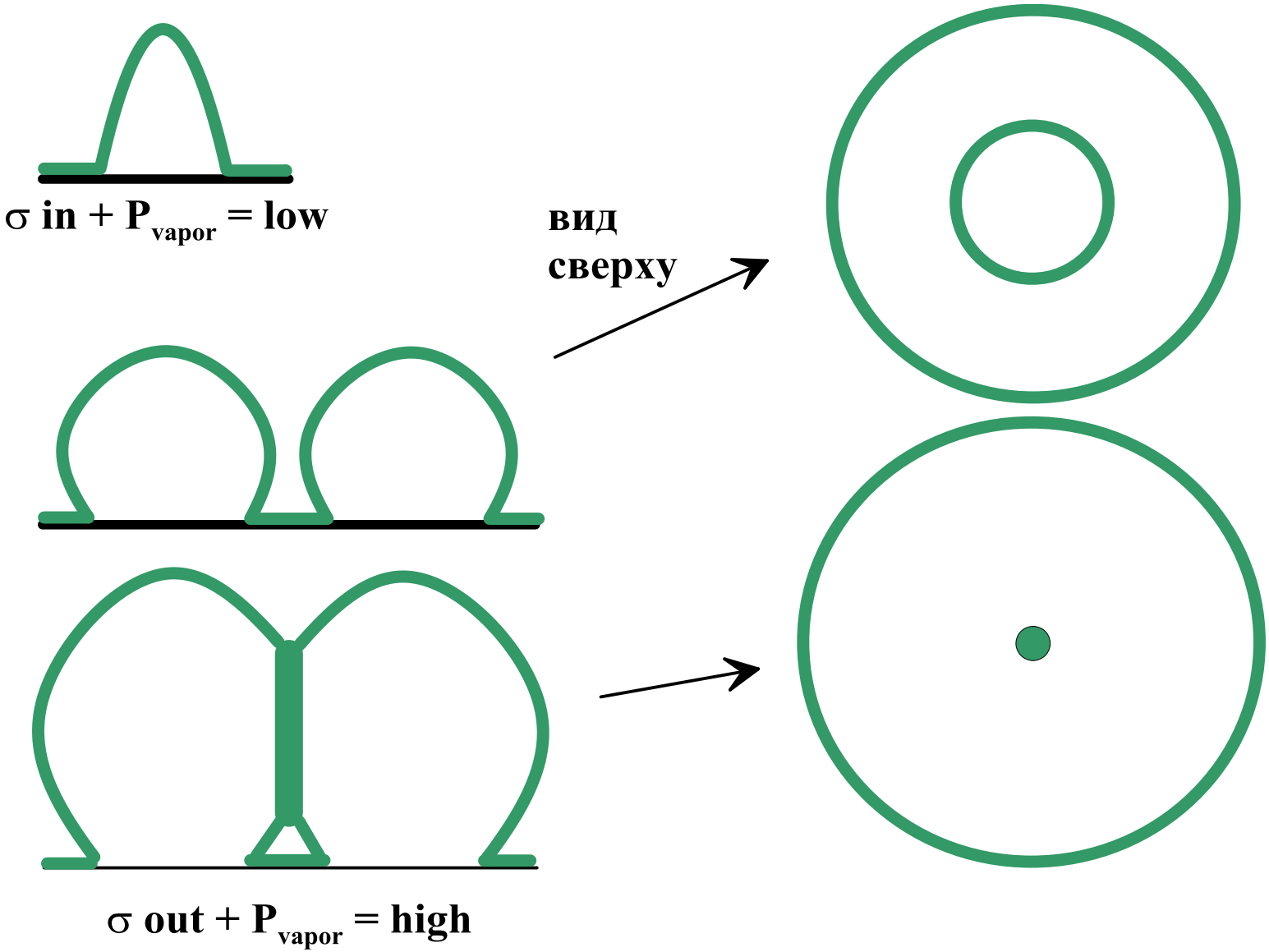

Focusing conditions:

- fluence
- radius of focal spot RL
- $R_L >> \lambda$
- $R_L \sim \lambda$

Kohmura,Zhakhovsky,..,INA,..,
Appl.Phys.Lett. v.112, 123103 (2018)

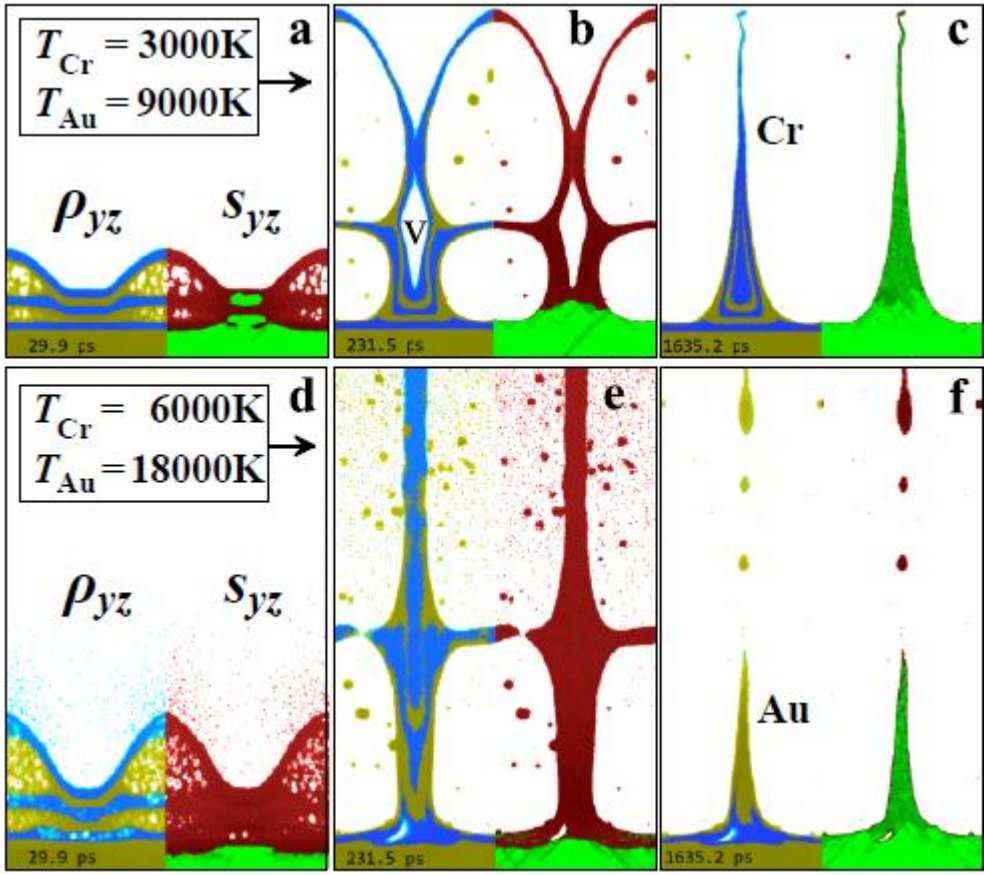

MD simulation of hard x-ray toroidal impact onto multilayer Au-Cr structure on Si mount done by V.V. Zhakhovsky

- beam structure:
- Gaussian
- Hermite-Gaussian
- Laguerre-Gaussian
- Spiral Fresnel Zone Plate (SFZP) – toroidal intensity distribution

Laser-matter interaction

- **Targets**: bulk targets, film targets
- Thin films – thick films
- Free standing films, supported films

- Laminates

- Nanoparticles formation
- Powders, sintering, dynamic throwing
- Porous media, compactification

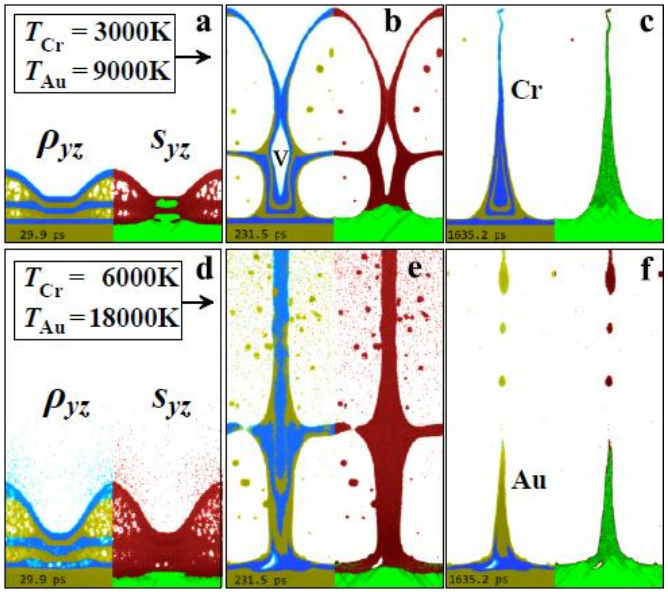

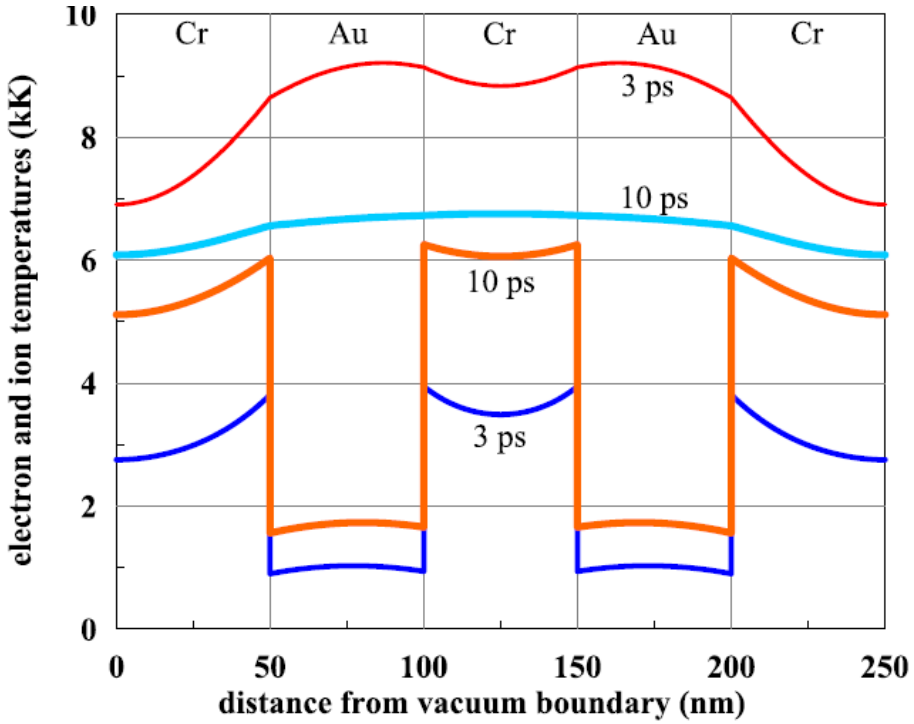

5-th layer Au-Cr laminate.
Effects of two-temperature stage:
Electron-ion coupling parameter is ten times higher in Chromium

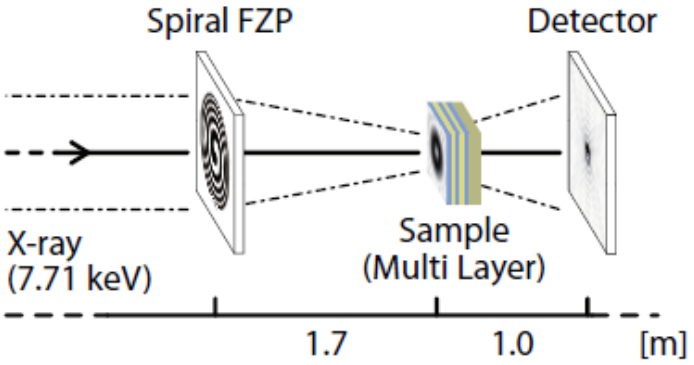

FIG. 1. Schematic view of SACLA nano-structuring experiment. The SFTP was introduced to create a focused x-ray vortex. The specimen was placed at the focal plane of th SFZP. A phosphor-coupled CCD camera was used to moni tor transmitted images of the specimen. The SFZP and th specimen were in vacuum and in room temperature durin the experiment.

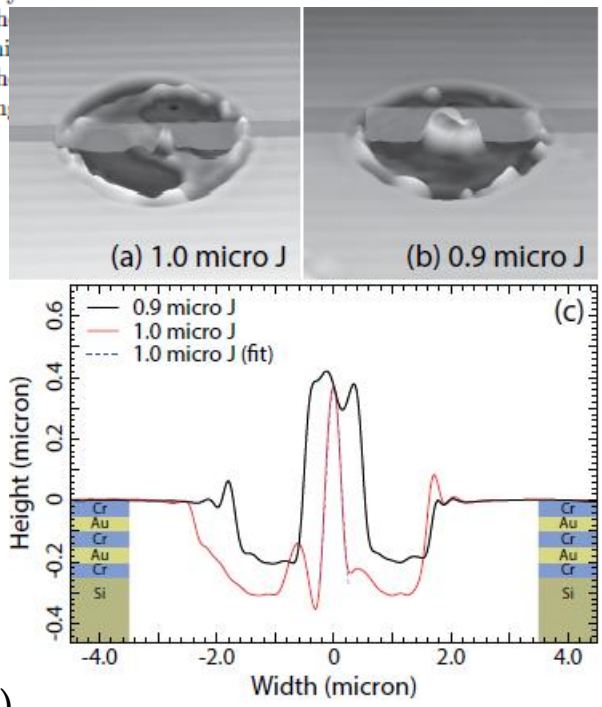

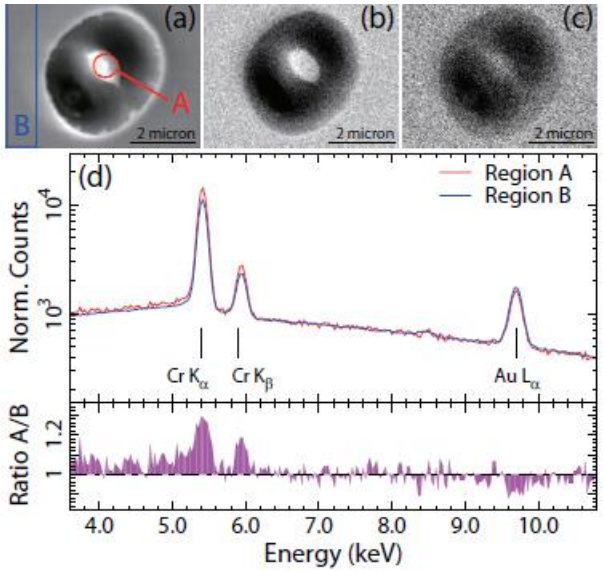

FIG. 3. (a) SEM image of the ablated spot by the 0.9 μJ pulse [Fig. 2(b)] with the electron-accelerating voltage and the magnification factor of 15 kV and ×20000, respectively. (b) Band-limited Cr $K_{\alpha 1,2}$ image, and (c) Au $L_{\alpha 1,2}$ image. (d) The upper panel shows the energy spectra from regions

Kohmura,Zhakhovsky,..,INA,..,
Appl.Phys.Lett. v.112, 123103 (2018)

Nano-structuring of multi-layer material by single x-ray vortex pulse with femtosecond duration

Yoshiki Kohmura,[1] Vasily Zhakhovsky,[2,3] Dai Takei,[4,1] Yoshio Suzuki,[5] Akihisa Takeuchi,[6] Ichiro Inoue,[1] Yuichi Inubushi,[6,1] Nail Inogamov,[3] Tetsuya Ishikawa,[1] and Makina Yabashi[1,6]

Laser-matter interaction

- **Targets**: bulk targets, film targets
- Thin films – thick films
- Free standing films, supported films
- Laminates

- # Nanoparticles formation

  Nanoparticles are formed thanks to Rayleigh-Taylor instability, see movie

- Имеется большое количество экспериментального характера
- Теоретическая работа и моделирование началась несколько лет назад, на сегодня имеются только две группы: **Поварницын, Итина, Левашов** в ИВТАНе и **Л. Жигилей**, США, унив. Вирджинии

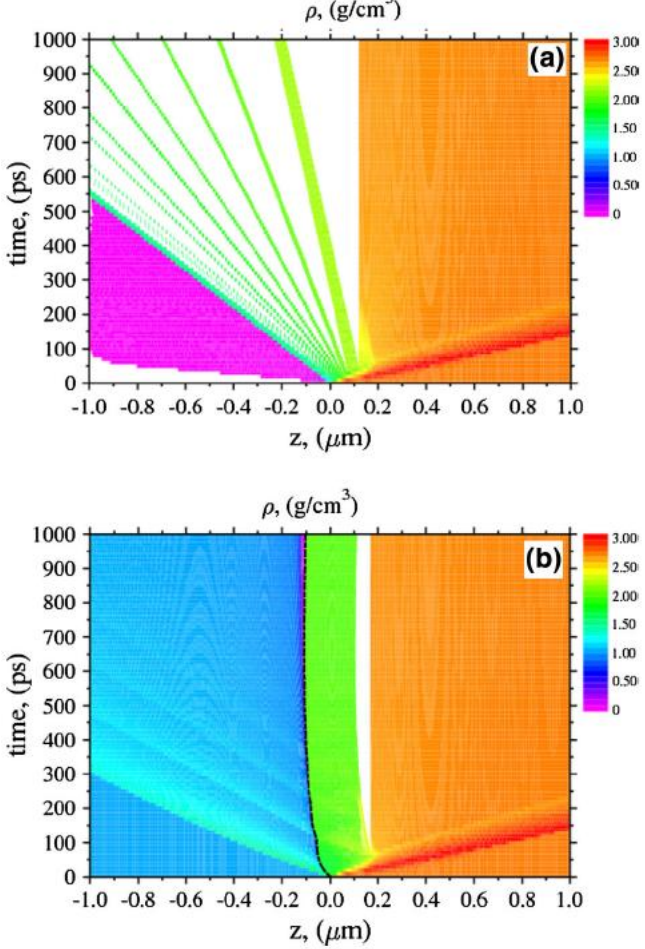

Fig. 1 Space–time diagram of density distribution. Al target ablation in vacuum—(**a**) and in water—(**b**) for $F = 1$ J/cm^2. *Dashed* (*black*) curve is the aluminum–water interface

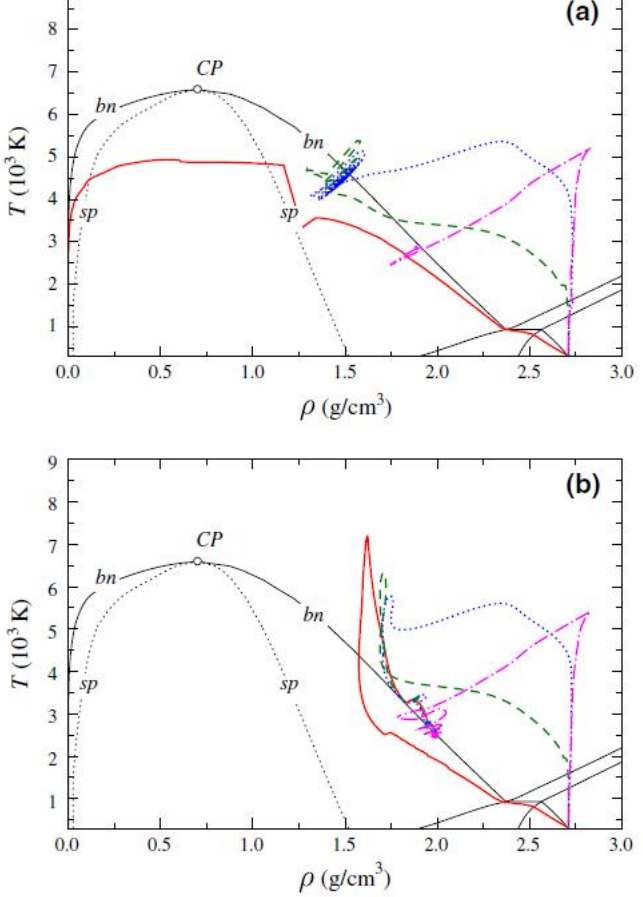

Fig. 2 Phase diagram of Al and thermodynamic trajectories of 1 nm (*solid red curve*), 5 nm (*dashed green curve*), 10 nm (*dotted blue curve*) and 50 nm (*dash-and-dot purple curve*) layers for Al target ablation in vacuum—(**a**) and in water—(**b**) for $F = 1$ J/cm^2. *CP* is the critical point, *bn* is binodal, *sp* is spinodal

Appl. Phys. A
DOI 10.1007/s00339-014-8319-1

Hydrodynamic modeling of femtosecond laser ablation of metals in vacuum and in liquid

Mikhail E. Povarnitsyn · Tatiana E. Itina

Received: 4 November 2013 / Accepted: 11 February 2014
© Springer-Verlag Berlin Heidelberg 2014

2T-HD 1D simulation results -1

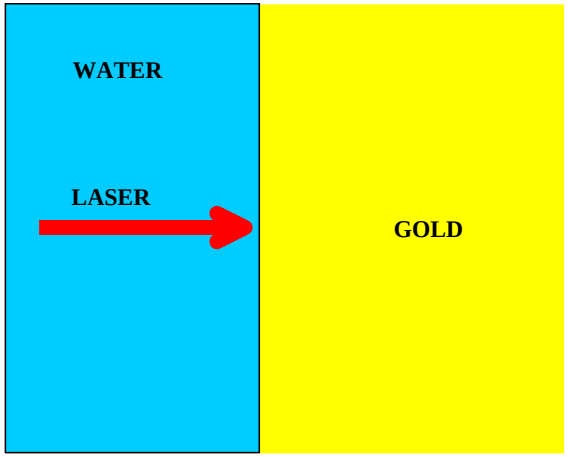

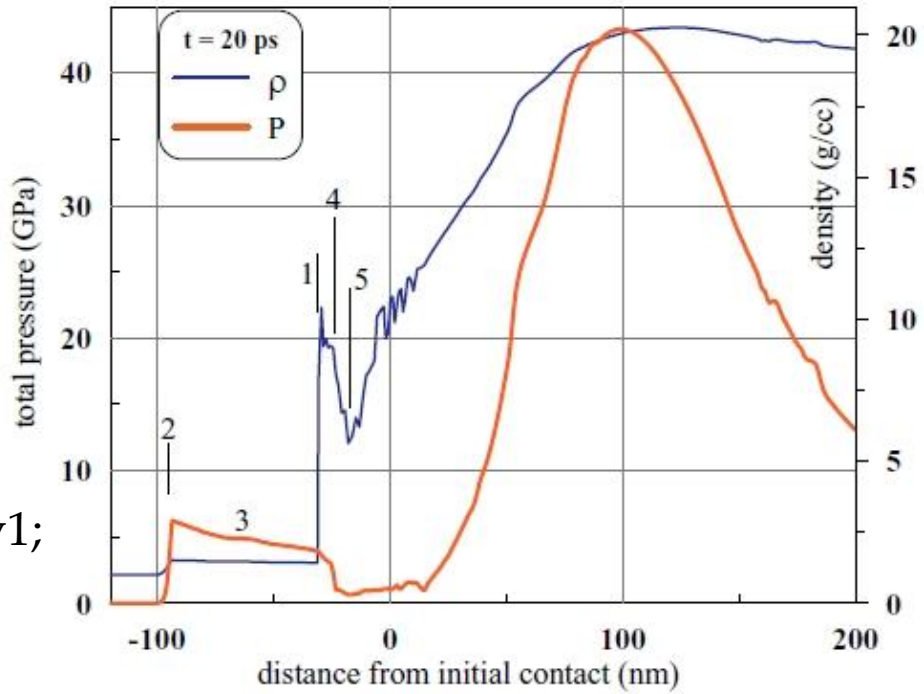

INA,Zhakhovsky,Khokhlov, arXiv:1803.07343v1;
ЖЭТФ, т.154,вып.1(2018)-принято в печать
AIP Proc. accepted (2018)

At the left side: Scheme of fs-laser action through water on gold. Intensities are below optical breakdown of water. At the right: Instant profiles of density (blue curve) and pressure (orange curve) at t = 20 ps after fs-laser action. The label 2 shows instant position of shock in water, 3 is a layer of shock compressed water, 1 is the contact between water and Au. The layer between the digits 1 and 5 is the ATMOSPHERE 4 made from Au. It is formed as a result of deceleration of the unloading Au by water. The molten Au continues up to the depth x=180 nm. Fluctuating region on the density profile to the right side relative to the label 5 (x~0) presents the layer where nucleation and development of two-phase liquid-vapor Au continue.

2T-HD 1D simulation results -2

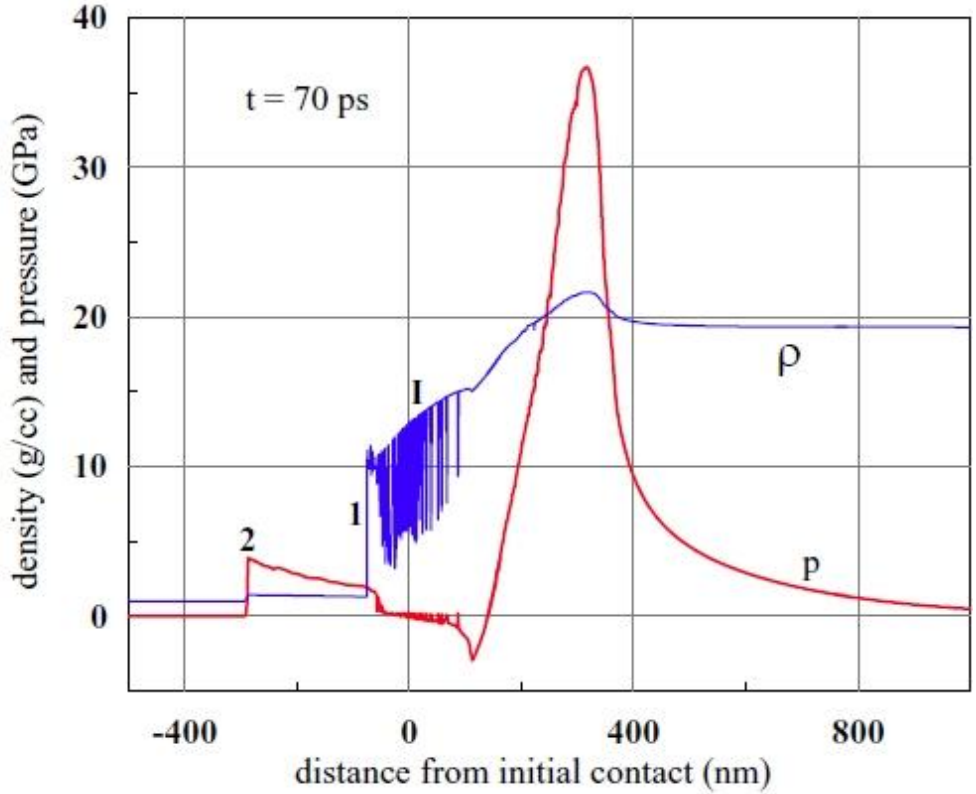

Continuation of the run shown in previous page, here t=70 ps. Absorbed energy F_{abs} is 400 mJ/cm^2, duration 100 fs. F_{abs} four times overcomes nucleation threshold. Therefore a wide zone I of nucleation (transforming in two-phase mixture) is formed. The thermodynamic states corresponding to this region are located near critical point. 2 is shock in water, 1 is the contact. Compression wave propagates to the right into bulk of Au. Gradually it becomes steeper and steeper and overturns forming weak (p is less than bulk modulus) shock in Au

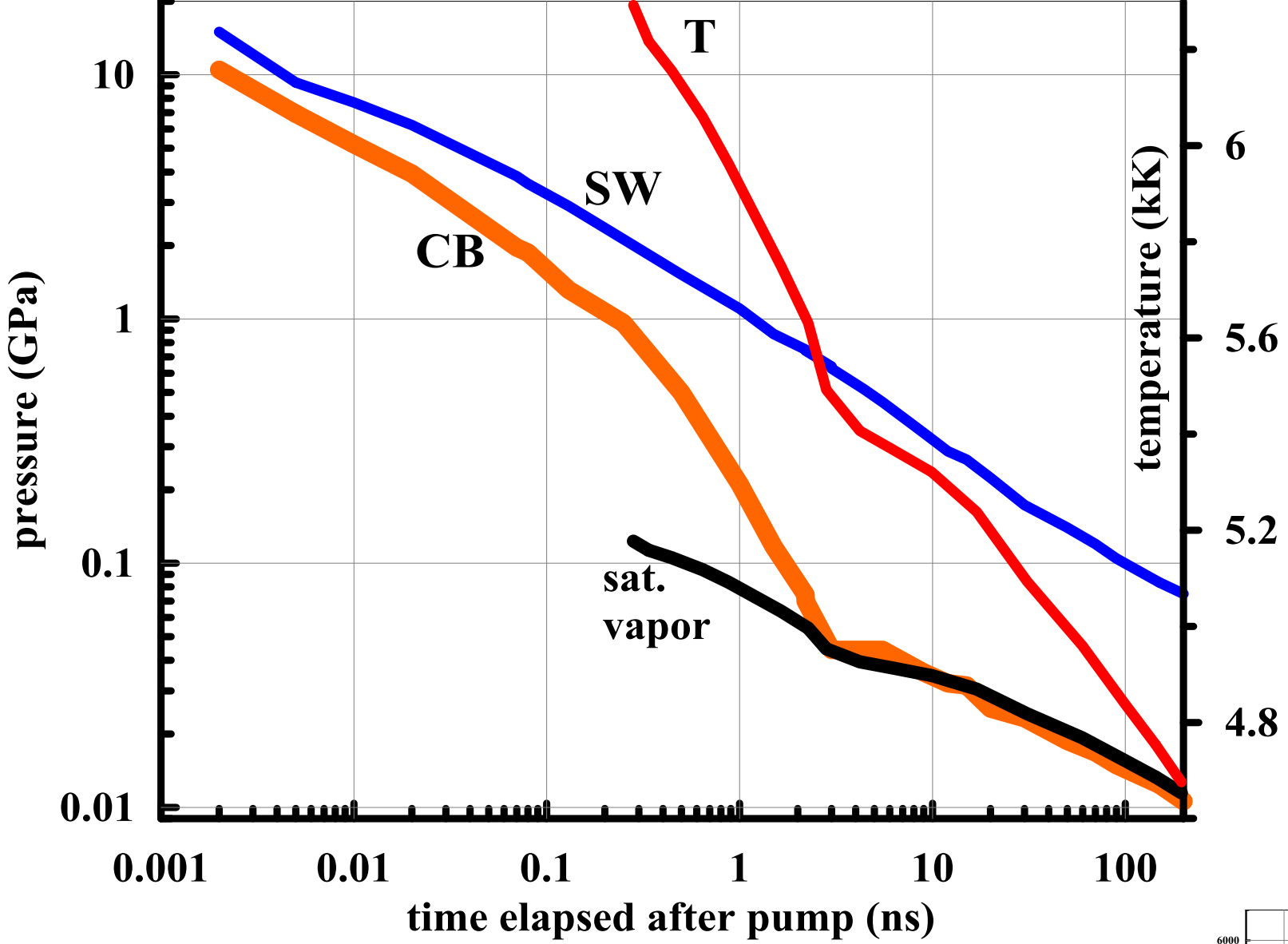
T
SW
CB
sat.
vapor
pressure (GPa)
temperature (kK)
time elapsed after pump (ns)
10
1
0.1
0.01
0.001
0.01
0.1
1
10
100
6
5.6
5.2
4.8

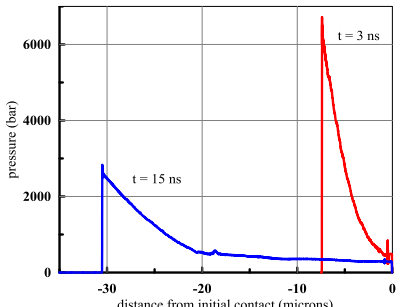
t = 3 ns
t = 15 ns
pressure (bar)
6000
4000
2000
0
-30
-20
-10
0

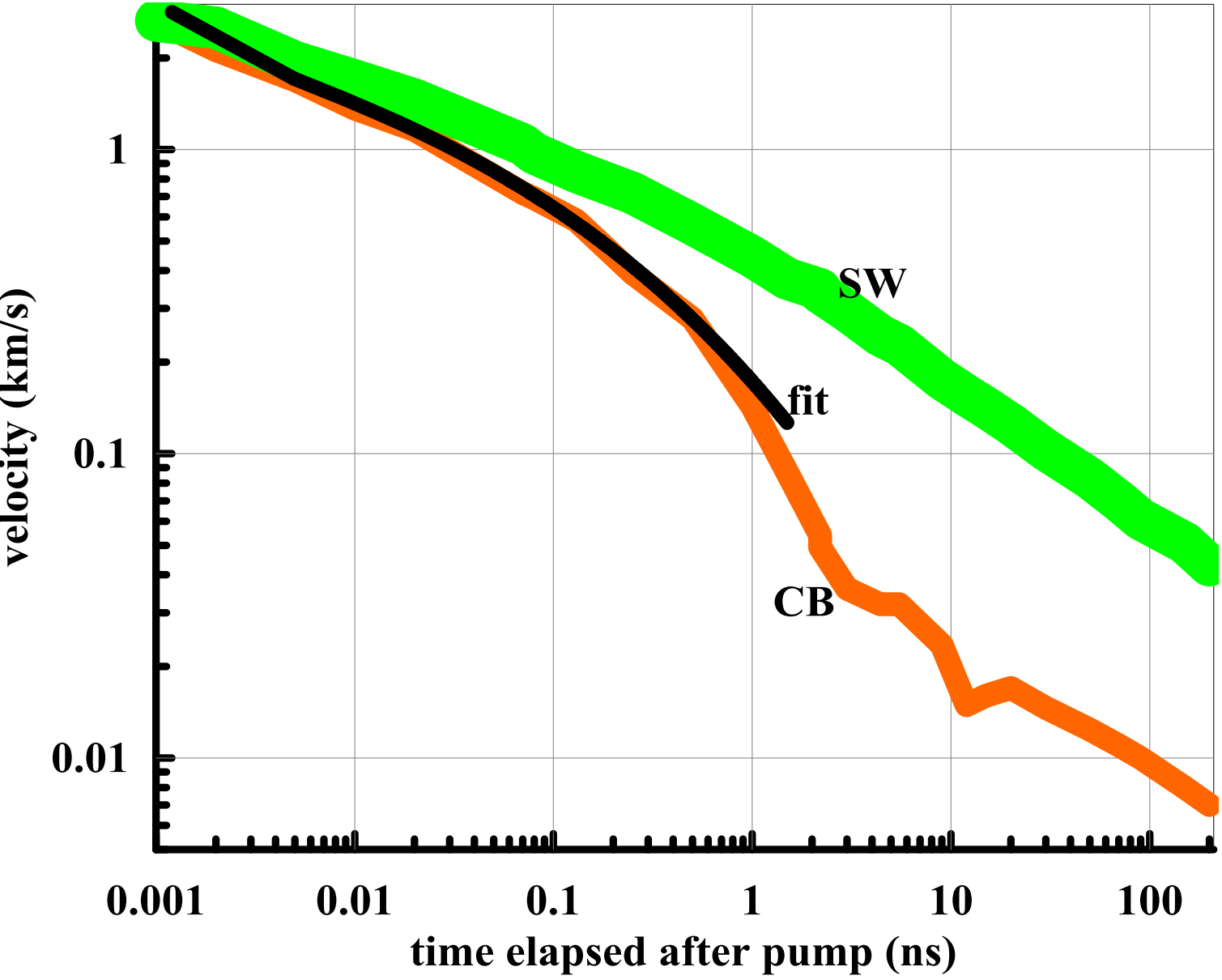

Deceleration from contact velocity→ calculation of linear RTI

$$\gamma = \sqrt{(2k^2\nu)^2 + g\,k\,\mathrm{At} - k^3\sigma/(\rho_A + \rho_w)} - 2k^2\nu.$$

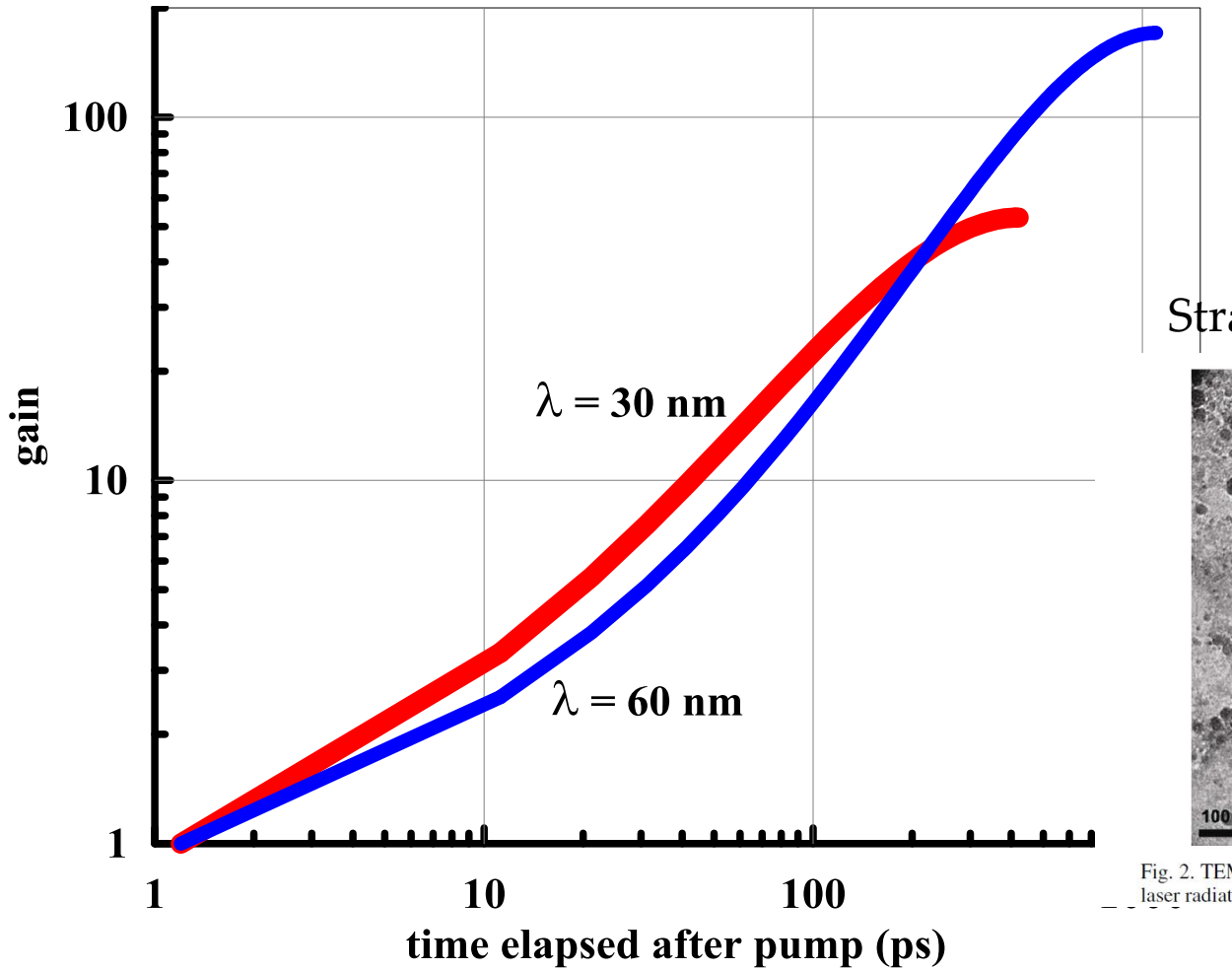

Stratakis et al., Opt.Express, 2009

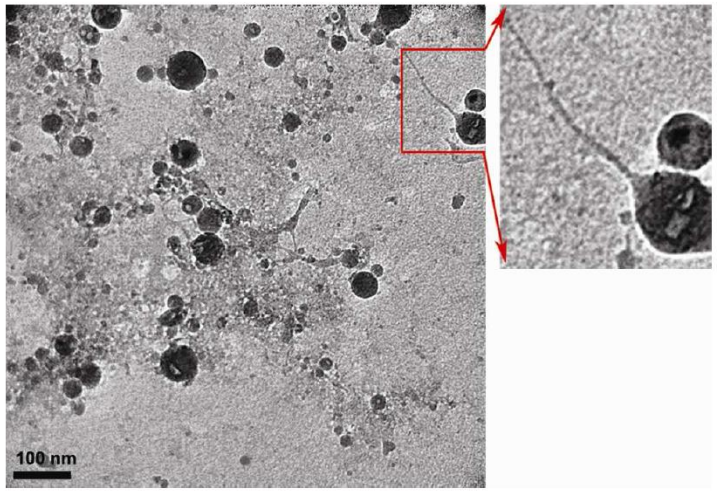

Fig. 2. TEM view of nanoparticles generated via ablation of a bulk Al target in ethanol us
laser radiation.

Viscosity of molten gold, surface tension of molten gold

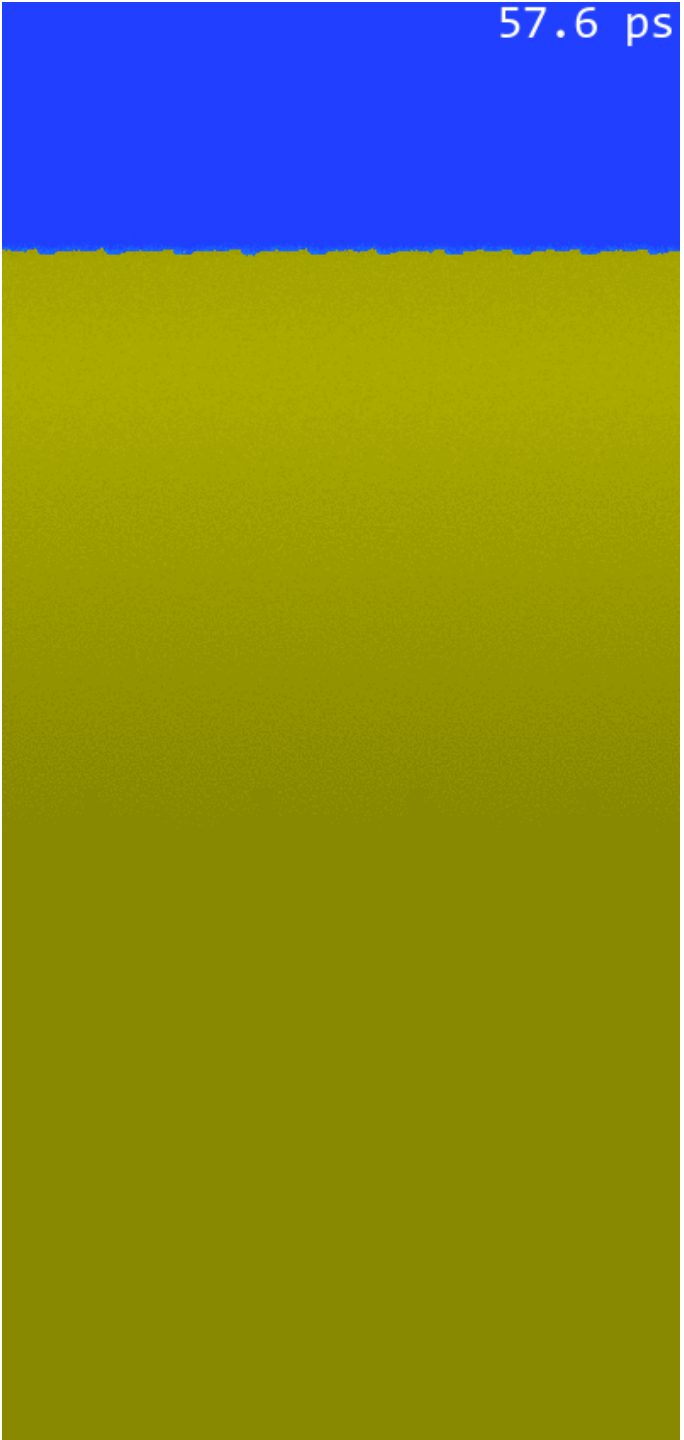

The key phenomena are:
gold (Au, yellow) is irradiated from above through blue water.
Hot Au expands into H2O.
Irradiation causes (1) nucleation and foaming in Au, (2) the layer of Au (= atmosphere) decelerated by H2O appears. Under H2O pressure the cavities in a foam collapse.
(3) there is “accretion” of foam onto atmosphere.
(4) deceleration of atmosphere leads to Rayleigh-Taylor instability

SCIENCE ADVANCES | RESEARCH ARTICLE

APPLIED PHYSICS

Dynamic fracture of tantalum under extreme tensile stress

Bruno Albertazzi,[1,2*] Norimasa Ozaki,[1,3*] Vasily Zhakhovsky,[4,8*] Anatoly Faenov,[3,5] Hideaki Habara,[1,3] Marion Harmand,[6] Nicholas Hartley,[1,7] Denis Ilnitsky,[4,8] Nail Inogamov,[4,8] Yuichi Inubushi,[9,10] Tetsuya Ishikawa,[10] Tetsuo Katayama,[9,10] Takahisa Koyama,[9] Michel Koenig,[2,5] Andrew Krygier,[6] Takeshi Matsuoka,[5] Satoshi Matsuyama,[1] Emma McBride,[11,12] Kirill Petrovich Migdal,[4] Guillaume Morard,[6] Haruhiko Ohashi,[9] Takuo Okuchi,[13] Tatiana Pikuz,[3,5] Narangoo Purevjav,[13] Osami Sakata,[14] Yasuhisa Sano,[1] Tomoko Sato,[15] Toshimori Sekine,[15,16] Yusuke Seto,[17] Kenjiro Takahashi,[3] Kazuo Tanaka,[1,3] Yoshinori Tange,[9,18] Tadashi Togashi,[9,10] Kensuke Tono,[9,10] Yuhei Umeda,[15] Tommaso Vinci,[2] Makina Yabashi,[10] Toshinori Yabuuchi,[1,10] Kazuto Yamauchi,[1] Hirokatsu Yumoto,[9] Ryosuke Kodama[1,5,19]

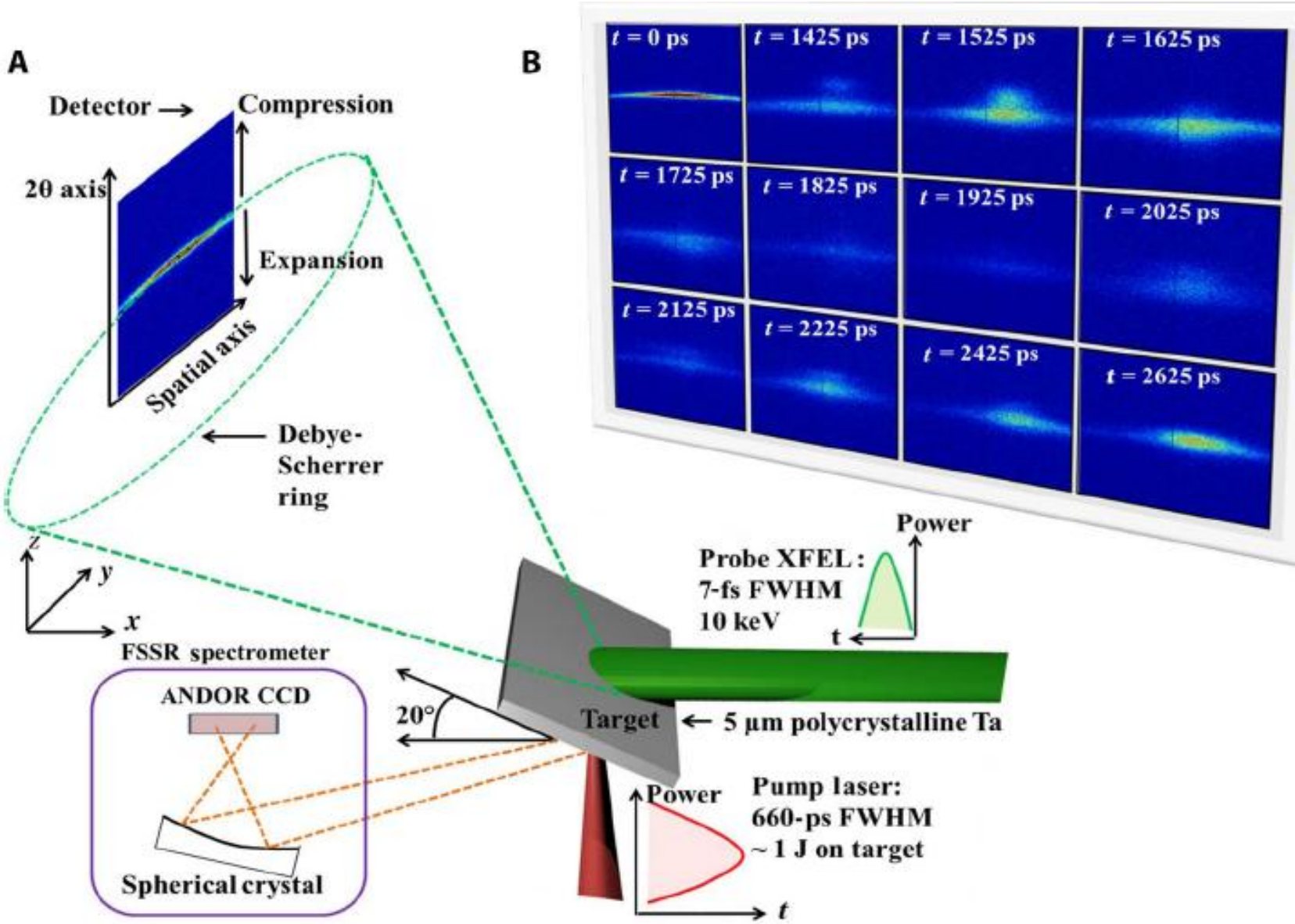

The pump-probe experiment at SACLA. (**A**) Experimental configuration, where a 5-μm-thick polycrystalline Ta sample is compressed by

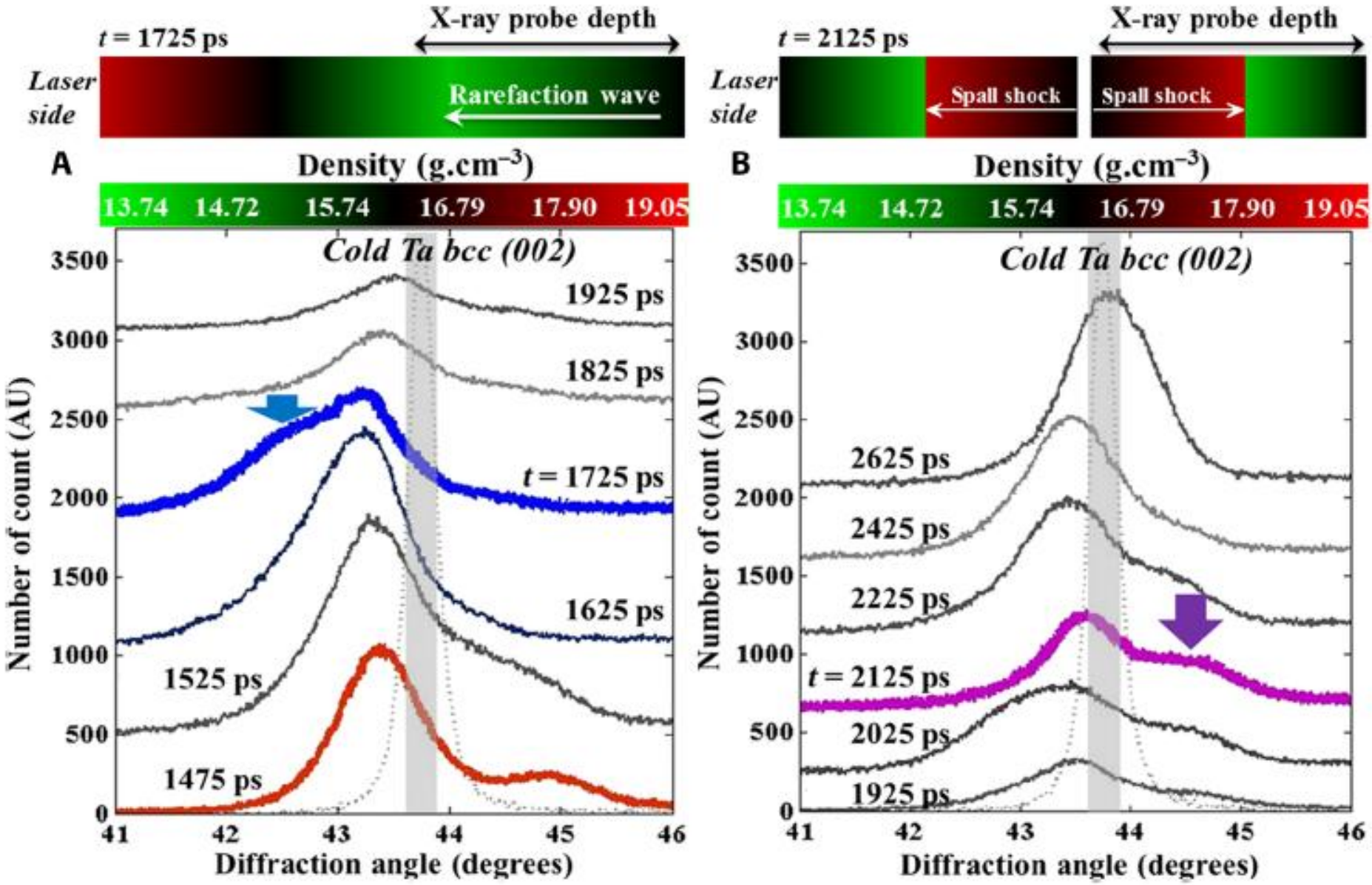
t = 1725 ps
X-ray probe depth
Laser side
Rarefaction wave
A
Density (g.cm−3)
13.74 14.72 15.74 16.79 17.90 19.05
Cold Ta bcc (002)
1925 ps
1825 ps
t = 1725 ps
1625 ps
1525 ps
1475 ps
Number of count (AU)
Diffraction angle (degrees)
t = 2125 ps
X-ray probe depth
Laser side
Spall shock
Spall shock
B
Density (g.cm−3)
13.74 14.72 15.74 16.79 17.90 19.05
Cold Ta bcc (002)
2625 ps
2425 ps
2225 ps
t = 2125 ps
2025 ps
1925 ps
Number of count (AU)
Diffraction angle (degrees)

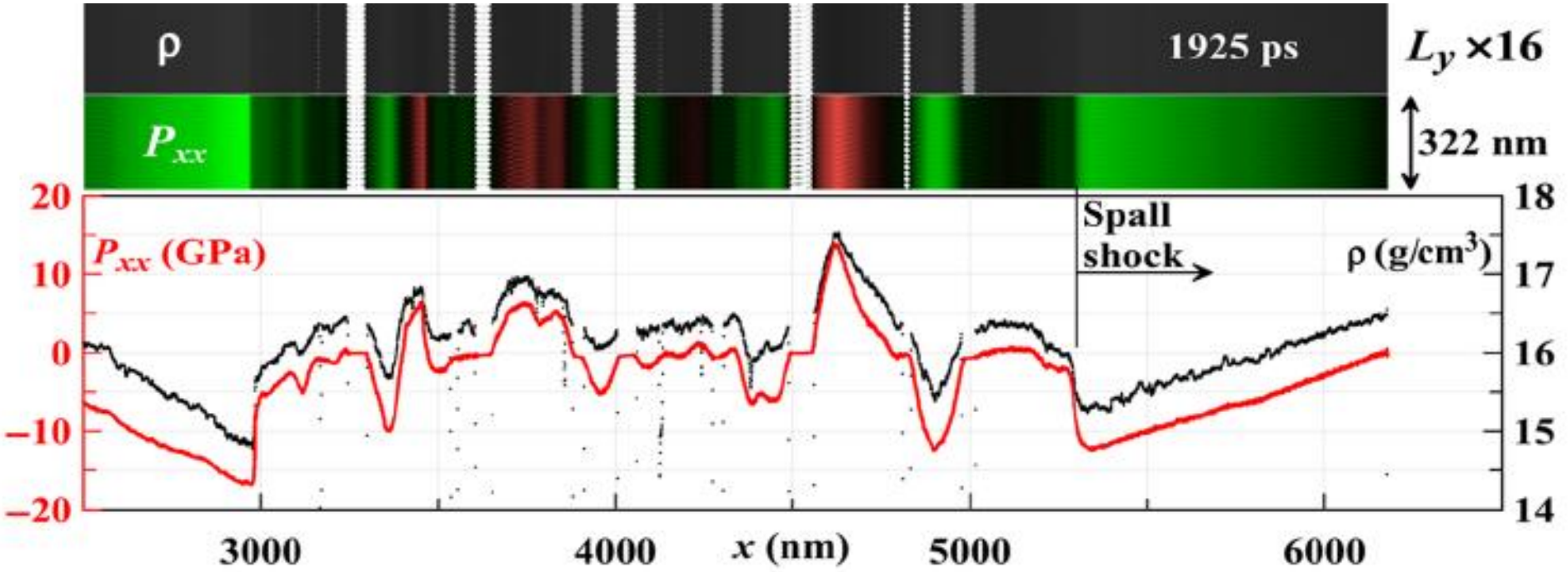
ρ
1925 ps
L_y ×16
P_{xx}
322 nm
20
10
0
−10
−20
P_{xx} (GPa)
Spall
shock
ρ (g/cm^3)
18
17
16
15
14
3000
4000
x (nm)
5000
6000

Our team and main connections

- Landau Institute for Theoretical Physics, Department of Lasers and Plasma
- Joint Institute for High Temperatures, Department of Laser Plasma
- Dukhov Research Institute of Automatics, Center for Fundamental and Applied Researches
- Kansai Photon Science Institute, X-ray Laser Group
-

Our team and main connections (continuation)

- Institute of Automation and Control Processes, Laboratory of high-precision optical methods of measurement
- Lebedev Physical Institute, Division of Quantum Radiophysics (DQRP)
- Munich University of Applied Sciences, Lasercenter
- и др.

Conclusions

- Very different laser sources may be used for surface structuring, nanoparticles production, and sintering of powders. They differ in wavelengths, fluences, and durations. Focusing conditions (Gaussian or non-Gaussian beams), diffraction conditions λ/R_L may be varied. Shot rate varies from single shot to many MegaHertz repetition rates.

Conclusions – continuation

- We developed physical models which allows to combine different codes to describe particular situation. These codes are: two-temperature Lagrangian hydrodynamics code; radiation propagation code solving Helmholtz equation; molecular dynamics code together with Monte-Carlo subroutine allowing to include electron heat conduction in metals; SPH code adapted for multiprocessors supercomputers; DFT packages (Elk, VASP etc.) for quantum mechanical simulations

Thank you for your kind attention !

The review is based on the papers listed

- B.J. Demaske et al., Ablation and spallation of gold films irradiated by ultrashort laser pulses, Phys. Rev. B 82, 064113 (2010) [5 pages].
- M.B. Agranat, S.I. Anisimov, S.I. Ashitkov et al., Strength properties of an aluminum melt at extremely high tension rates under the action of femtosecond laser pulses, JETP Lett. 91(9), 471-477 (2010).
- V.V. Zhakhovskii, N.A. Inogamov, Elastic-plastic phenomena in ultrashort shock waves, JETP Lett. 92(8), 521-526 (2010).
- N.A. Inogamov, V.V. Zhakhovsky, V.A. Khokhlov, and V.V. Shepelev, Superelasticity and the Propagation of Shock Waves in Crystals, JETP Lett. 93(4), 226-232 (2011).
- V.V. Zhakhovsky et al., Two-zone elastic-plastic single shock waves in solids, Phys. Rev. Lett. 107, 135502 (2011).
- S.I. Ashitkov, N.A. Inogamov, V.V. Zhakhovsky et al., Formation of Nanocavities in Surface Layer of Aluminum Target irradiated by Femtosecond Laser Pulse, JETP Lett. 95(4), 176-181 (2012).
- Yu.V. Petrov, N.A. Inogamov, and K.P. Migdal, Thermal Conductivity and the Electron–Ion Heat Transfer Coefficient in Condensed Media with a Strongly Excited Electron Subsystem, JETP Lett. 97(1), 20-27 (2013).
- B.J. Demaske, V.V. Zhakhovsky, N.A. Inogamov, I.I. Oleynik, Ultrashort shock waves in nickel induced by femtosecond laser pulses, Phys. Rev. B 87, 054109 (2013).
- N.A. Inogamov and V. V. Zhakhovskii, Formation of Nanojets and Nanodroplets by an Ultrashort Laser Pulse at Focusing in the Diffraction Limit, JETP Lett. 100(1), 4-10 (2014).
- N.A. Inogamov, V.V. Zhakhovskii, and V.A. Khokhlov, Jet Formation in Spallation of Metal Film from Substrate under Action of Femtosecond Laser Pulse, Journal of Experimental and Theoretical Physics (JETP) 120(1), 15-48 (2015).
- N.A. Inogamov, V.V. Zhakhovsky, K.P. Migdal, Laser-induced spalling of thin metal film from silica substrate followed by inflation of microbump,
- Applied Physics A: Material Science and Processing 122, 432 (9 pages) (2016).
- A. Kuchmizhak, O. Vitrik, Yu. Kulchin, D. Storozhenko, A. Mayor, A. Mirochnik, S. Makarov, V. Milichko, S. Kudryashov, V. Zhakhovsky, N. Inogamov,
- Laser printing of resonant plasmonic nanovoids, Nanoscale 8, 12352-12361 (2016).
- N. A. Inogamov, V. V. Zhakhovsky, V. A. Khokhlov, Yu. V. Petrov, and K. P. Migdal, Solitary Nanostructures Produced by Ultrashort Laser Pulse,
- Nanoscale Research Letters 11, 177 (2016).
- P.A. Danilov, D.A. Zayarny, A.A. Ionin, S.I. Kudryashov, A.A. Rudenko, A.A. Kuchmizhak, O.B. Vitrik, Yu.N. Kulchin, V.V. Zhakhovsky, N.A. Inogamov,
- Redistribution of a Material at Femtosecond Laser Ablation of a Thin Silver Film, JETP Lett. 104(11), 759-765 (2016).
- X. W. Wang,1 A. A. Kuchmizhak,1, 2, 3, X. Li,1 S. Juodkazis,1, 4 O. B. Vitrik,2, 3 Yu. N. Kulchin,3 V. V. Zhakhovsky,5, 6 P. A. Danilov,3, 7 A. A. Ionin,7 S. I. Kudryashov,3, 7, 8 A. A. Rudenko,7 and N. A. Inogamov6, Laser-induced Translative Hydrodynamic Mass Snapshots: non-invasive characterization and predictive modeling via mapping at nanoscale, Phys. Rev. Appl. (in press)